

## REMARKS

The following remarks are submitted to address issues raised in the Official Actions mailed March 9 and September 9, 2004; and to provide the Summary of Interview, which took place by telephone on December 17, 2004.

The applicant clarifies that the remarks made in this communication are being made without counsel of attorneys. All previous powers of attorney granted in the matter of this patent application were revoked by the applicant on November 22, 2004.

### Amendments to claim 5

The applicant further indicates to this office that per the agreement to strike the word “therapeutic” from all claims as submitted in the applicant’s response and amended claims mailed on June 9, 2004; and upon discovery that previously retained counsel twice neglected to strike the word “therapeutic” from claim number 5; applicant asks that said claim number 5 likewise be amended to read:

5. (Original) The method of claim 4, further comprising the step of determining a refractive index of the electromagnetic radiation through the in-vivo tissue by dividing the speed of light in a vacuum by the speed of light in in-vivo tissue, wherein dividing one ~~therapeutic~~ resonant frequency determined for the genomic material surrounded by air by the refractive index for in-vivo tissue yields one of the ~~therapeutic~~ resonant frequencies for the genomic material surrounded by in-vivo tissue.

## **SUMMARY OF INTERVIEW**

The applicant thanks Examiner Marschel and Supervisor Woodward for their time given in the telephonic interview conducted with the applicant on December 17, 2004. Following is a summary of the interview.

The applicant briefly explained the reasons for the revocation of attorney action taken in November 2004, and advised the examiner that applicant was unable to review and approve the response sent to the examiner on June 9, 2004 by counsel retained at that time. This problem was caused by counsel's failure to submit the material to the applicant with enough lead time to approve it. Applicant received counsel's version of the response four hours before it was sent to this office. The applicant was working away from her office, and had no opportunity to read or review that document. The applicant feels counsel's negligence on this matter resulted in a potentially serious misunderstanding by the examiner on one major point of discussion, that regarding resonance. (This is further addressed in the applicant's full response included with this paper. Confirmation of the applicant's circumstances is also submitted with this paper as an attached document).

In the phone interview, applicant further advised the examiner of intense research and developments in the closely related fields of bioelectromagnetics and biophysics, including but not limited to: application of electric fields for medical diagnostics and devices; bioeffects of pulsed microwaves, millimeter waves and nonthermal plasmas; biological decontamination by pulsed electric fields; plasma-based sterilization; and biomedical application of plasmas. The applicant stated that she has experienced numerous inquiries from parties wanting to use her method for commercial applications and/or research, and asked that her application might come under timely consideration by the office in view of the long period (nearly four years) since submission of the nonprovisional application.

The applicant addressed the office response from 9-9-04, top of page 3 (and from 3-9-04, bottom of page 3), both of which state: "The Board also stated that although the level of skill in molecular biology is high, the results of experiments in genetic engineering are unpredictable." The applicant clarified that the method described in the submitted application has absolutely no relationship to genetic engineering or related process, in the sense that the phrase "genetic engineering" is currently defined and understood in the scientific community.

The rejections of the examiner under 35 U.S.C. § 112, first paragraph, regarding radio metallic antenna science and how it may compare to DNA or RNA molecular chain resonant response were discussed. The applicant pointed out that there are numerous mechanisms of resonant excitation in chain biomolecules that are considerably different in nature than those occurring in metallic antennas, and that these mechanisms do not have parallel concepts to radio antenna theory. She also pointed out that there would be differences in response from metallic antennas as compared to chain nucleic acids due to the significant differences in the material, and offered that a strict direct analogies between living DNA and metallic radio antenna response would therefore be inappropriate for purposes of analyzing this method. The examiner then reviewed principles of resonance, and stated that the method as presented in claim 1 did not seem that far removed from radio antenna resonance, and that the difference in material would be irrelevant. He also pointed out that DNA is conductive, which would also be similar to metallic antennas, and stated that the difference in material between a metallic antenna and DNA is irrelevant. Agreement was not reached on this particular matter during the course of the phone interview.

The applicant indicated that there exists a body of material in the field of biophysics that could help address this and other issues relating to the enablement objections in the previous two office actions. It was agreed that it would be more productive to present this material in written form in the next response from the applicant, and the examiner also suggested that submission of case studies and other information to establish predictability would be helpful to him in his considerations.

The applicant also pointed out that a claim from a previously granted U.S. patent (# 6,060,293, submitted in the prior art material) includes chain molecule length in its mathematical formula to compute an electromagnetic resonant frequency (the formula is not the same as in the application under consideration). This would establish that determination of chain molecule length has previously been allowed in a patent. It was agreed that the applicant would submit the relevant details from that patent in her next response.

The examiner kindly verified that the applicant will need to send in a request and payment for extension of the current statutory response period.

Remainder of this page is left blank.

## **RESPONSE**

### **Case study results using this frequency method**

The applicant submits the following case results as evidence of efficacy, predictability and repeatability of the method under consideration.

#### **Example 1.**

A healthy and physically active 40-year old man diagnosed by physicians with a case of Barmah Forest disease (a mosquito-transmitted viral disease endemic to certain regions of southern Asia), used a frequency-emitting device with numerous frequencies in an attempt to alleviate the clinical effects of the disease. The effects included severely debilitating arthritis-type conditions, and significant alteration of iron metabolism and levels in the blood. Lab results of blood iron levels and related factors are used by physicians to diagnose this viral disease. The patient was unable to work at his previous full-time job because of the disease. The iron level at the time of diagnosis was 10  $\mu\text{mol/L}$  (at the very bottom of reference range), and remained near that level after his initial use of the device and commonly-used frequencies. The debilitating arthritis symptoms likewise continued without positive resolution, indicating the frequencies being used were not efficacious. The patient had been suffering in this manner for 10 months. The frequency protocol was then altered to consist of DNA-related numbers (as described in this application) for the full genome and several active genes of the virus. After the frequency protocol was changed, the patient experienced nearly full clinical recovery within two weeks, complete recovery shortly thereafter, and was able to resume his normal full-time heavy physical activity. The recovery was later confirmed by an iron test at 21.7  $\mu\text{mol/L}$ , which is in normal range. No other medical protocols were changed during the time that the DNA-related frequency program was used. The man remains fully recovered with complete and permanent absence of any disease symptoms. This case has been monitored for 5 years.

**Example 2.**

A healthy woman in her middle 30s was diagnosed with cervical cancer confirmed by presence of human papilloma virus, and underwent a hysterectomy procedure. Subsequent physical examinations showed continued presence of cancerous cervical lesions, and the patient was scheduled for a surgical procedure to remove them. Before that procedure took place, the patient had begun using a frequency emission device with numerous frequencies, in an effort to clear the condition. This initial effort did not result in successful clearance of the lesions. The frequency program was then changed to the DNA-related frequency (as described in this application) corresponding to human papilloma virus type 16. Six weeks after the commencement of use of the new frequencies, physical examination discovered a complete disappearance of all cervical lesions, and the surgery was cancelled. A subsequent blood test showed disappearance of the viral antibodies that had previously been present in the blood. Ongoing monitoring indicates continued absence of any cervical lesions. This case has been monitored for four years.

**Example 3.**

A middle-aged American man in his 30s had been diagnosed with AIDS, confirmed by HIV-1 viral load and CD4 cell counts. The use of various medical and integrative alternative protocols for a period of 6-7 years had been partially but not totally successful, and included use of frequency emission devices with various frequency programs. After a period of time the viral count gradually climbed to 220,000 copies/ml. The patient at this point in time began using a new set of frequencies, consisting of DNA-related numbers corresponding to certain components of the virus, as described in the method. There were no other changes initiated in his medical protocol at this time. Subsequent to the start and daily use of the new frequencies, a blood test three weeks later showed a virus count of 100 copies/ml. Another blood test three weeks afterwards reported a count of less than 50 copies/ml (the limit of sensitivity for that test). The latest and blood test (current to the date of this communication) shows a count of less than 50 copies/ml. This individual was not taking any anti-viral drugs during the period of time covering this report, and had not been taking any such drugs for a period for 3.5 years prior to use of

DNA-related frequencies as described in this application. This case continues to be carefully monitored.

**Example 4.**

In a case similar to example 3, an American woman diagnosed with AIDS confirmed by viral load and CD cell count lab tests. The patient has experienced a drop in viral load from 15,000 copies/ml to 80 copies/ml in a period of three months, using the same frequency program as the person described in example 3. This case continues to be carefully monitored.

**Example 5.**

This example addresses a community outbreak of what physicians described as contagious shingles also resembling chickenpox (itching, painful, oozing and sometimes bloody lesions), spreading among both adults and children via physical contact. Some individuals had been suffering severe symptoms for a period of 2-3 months. Patients had been prescribed anti-viral and anti-inflammatory drugs, but the drugs did little if anything to resolve the affliction. Some patients in near desperation sought alternative assistance and commenced use of a frequency emission device. That device was programmed with a number of frequencies available from public sources. Those frequencies had partial effects on part of the symptoms in a few but not all individuals, however the effects were not permanent and did not resolve the affliction. The frequency program was later changed to use of DNA-related frequencies (as described in this application). The change in effect on the patients was immediately noticeable. For some individuals, especially the children, the itching and pain was largely resolved within 2-3 hours. For most others, the lesions were noticeably healing within 24-72 hours. A total of 30 individuals from the community were treated, and the outbreak was stopped. Many of the patients only needed one frequency session for the problem, and 7 of the more severely afflicted persons needed 2 or 3 sessions.

**Example 6.**

An elderly woman was hospitalized and diagnosed with a lung infection caused by the bacterium *Gordona sputi*, which became totally unresponsive to antibiotics or any other medical protocols. Her physicians told her they could do nothing more, advised her to prepare for death, and sent her home from the hospital. The woman began use of a frequency device using commonly available frequencies characterized by many reports as having anti-bacterial effects. The infection was not resolved and the illness continued. The program was then changed to use of four DNA-related frequencies that correlate with important components of this bacteria (the genome has not been decoded, thus the frequency related to the full genome could not be used). The infection was cleared within a short time span (1-2 weeks), the woman completely recovered, and has never experienced a relapse. This case has been followed for 3-1/2 years.

**Example 7.**

A 50 year old woman employed as a nurse in a hospital acquired a herpesvirus infection via contact with a patient. The infection manifested as the condition known as Herpes Whitlow, caused by human herpesvirus 1, and manifested on her hands. As is characteristic of infections from this virus, the clinical lesions would appear and then slowly heal over a period of approximately 10 days. The woman had been suffering from this condition for 7 years, and occasionally made it difficult for her to work in her profession. At the time of the most recent outbreak of lesions, she began using DNA-related frequencies (as described in this application). The lesions on her hands healed within three days, as compared to 14 days without use of this frequency method. The woman stated that use of non-DNA-related frequencies actually made the healing process take longer, than if she had done nothing at all.

**Example 8.**

Two American missionaries working in Africa had been fighting malaria infections on a continual basis, as is common in that region. Over a four-month period, they used a frequency emission device with numerous frequency sets. By the fourth month they were able to narrow down a successful outcome to a basic set of six frequencies that correlated with important



components of the causative organism *Plasmodium falciparum*. One specific result was seen in a man with the following history: day 1, a mid-morning initial Quantitative Buffy Coat test showed 89 malaria parasites per 200 white blood cells (WBCs), which is equivalent to 3,560 parasites per microliter of blood. Two sessions with the aforementioned DNA-related frequencies were received by the individual later that morning and in the late afternoon. On day 2 at 8 am, the same blood test showed 10 malaria parasites per 200 WBCs (or 400 per microliter), which constitutes an 80% parasite count reduction within less than 24 hours. These results were re-checked at 9 am, with the count being 7 malaria parasites per 200 WBCs (or 280 per microliter). A different lab test performed at the same time (blood smear), gave a result of 5 malaria parasites per 200 WBCs (or 200 per microliter). A further blood smear re-test later that morning at a second medical facility gave a result of 0 (zero) parasites per 200 white blood cells. The man also reported complete cessation of clinical symptoms (fever, body aches, headache) that same day. Tests on day 3 at 10 am gave the following results: Quantitative Buffy Coat, 7 malaria parasites per 200 WBCs (280 per microliter); blood smear, 5 malaria parasites per 200 WBCs (200 per microliter). Importantly, no anti-malaria drugs were taken during this period of frequency sessions.

Similar reductions of malaria parasite levels along with cessation of clinical symptoms were seen in several other people after using the DNA-related frequencies. Because reinfection from mosquitoes is an ongoing problem, it is not expected that use of this non-invasive technology would produce a permanent cure in humans; however, repeated use of relevant frequencies during episodes of reinfection could significantly reduce levels of the parasitic organism, and eventually reduce the cycle of reinfection in mosquitoes as well, if enough people were able to take advantage of the technology.

#### **Brief comments on case studies**

It should be noted that:

1. Case numbers 1, 2, 3, 5, 6, 7, and 8 demonstrated that desirable positive effects in laboratory and/or clinical results were achieved with DNA-related frequencies as calculated from the method presented in this application, as opposed to lack of such results with previously-

administered frequencies, thus proving specificity of action with the frequencies as calculated by the method shown in the application currently under consideration.

2. Case #4 (HIV-1) repeats the outcome shown in case #3 (also HIV-1), showing repeatability; and case #5 clearly demonstrates repeatability over a significant group of people with the same illness (n=30).

3. These cases reveal positive outcome against bacteria, viruses, and parasitic blood organisms, which indicates potential wide applicability to human disease conditions caused by those classes of pathogens.

#### **Considerations regarding previously granted patent**

The applicant would like to draw attention to U.S. Patent 6,060,293 granted May 9, 2000, titled "Resonant Driven Changes in Chain Molecule Structure", which was submitted as prior art in this application.

The abstract of this patent states that the invention relates to the application of electromagnetic or sound waves to resonantly affect the structure of chain molecules, including protein and nucleic acid chains. Briefly quoting the abstract: "The invention relates to the technical application of electromagnetic radiation such as microwaves and radiowaves and application of ultrasound to chain molecules...the technique is based on a new understanding of the underlying physical phenomenon and can also be applied to other chain molecules and biologically active biomolecules and tailored polymers such as...genomic chain molecules such as DNA and RNA."

Claim number 20 states in part: "A method according to claim 19, comprising: disintegrating the aggregates by applying high frequency energy from an external energy source;...applying high frequency energy to the fluid system correspond to the resonance frequency,  $\nu$ , of the twist mode of the chain molecule, said resonance frequency being estimated as  $\nu = [1/2\pi L][\text{sq root } (y/I)]$  where  $y$  is the torsion energy per inverse unit length, and  $L$  is the length of the backbone of the chain.

Claim number 24 further states in part: “A method according to claim 1, wherein the chain molecule is a molecule selected from the group consisting of...genomic chain molecules; artificial genomic chain molecules...”

Claim number 32 also states the aforementioned mathematical formula, previously shown in claim 20.

The applicant would like to point out it is clear that while the method described in this patent uses a mathematical formula that is different from the one used in the application currently under consideration, according to claims 20 and 32 it distinctly relies on a term in the equation which is the chain length of the biomolecule. It is also clear from claim 24 that such a chain molecule could be DNA or RNA, because genomic molecules can be made from DNA or in the case of certain viruses, RNA. It is therefore the applicant's understanding that use of the length of a DNA or RNA chain molecule has been allowed in a previously awarded patent. It is also evident that the concept and phenomenon of resonance relating in part to the length of a DNA or RNA molecule is allowed in that same patent. The applicant asks that these facts be taken into consideration to overcome the relevant parallel conceptual objections in the previous office actions, in the application currently being reviewed.

The applicant also points out that the computation of the chain length in the application now under consideration is more thorough than that stated in patent 6,060,293; in fact, that patent does not give any instructions at all regarding how to come up with a chain length of the various biomolecules addressed in the patent. Therefore, because the method in the application under consideration gives clear and specific instruction regarding the commonly accepted way of computing the length of a nucleic acid chain (contained in claims 1, 2, 15; and in the present specification page 10 lines 21-24 continued on page 11 lines 1-5), this particular calculation giving the chain length needed for further computation is even more clearly enabled to someone of ordinary skill in the art, than in the previously-granted patent.

#### **Regarding antenna considerations and wavelength calculation**

The Office Action dated 9-9-04, which reiterates reasoning from the Office Action of 3-9-04, maintains that use of a wavelength based on the length of a DNA or RNA chain “does not

include consideration of the coiled etc. complexity of such DNA or RNA in genomic material” (quoted from middle of page 3). It also cites concepts drawn from metallic antennas used in radio science technology.

The applicant thus points to the following information available from the scientific biophysics literature.

1. Metal antennas are very conductive materials, but DNA is an organic non-metallic molecule with a much smaller density of free electrons than metals. While the conductive characteristics of DNA are currently the subject of intense interest and research, there are no wide-ranging simple conclusions about its conductivity in all situations. A recent physics journal article reviews the state of research in this field, which comments that “the question of whether DNA is intrinsically conductive is an unsolved problem”, and teaches that “there are many factors that influence DNA conductivity”, a few of which are sequence, length of the molecule, morphological character of the molecule, environment of DNA as well as its microstructure, and other factors. Furthermore this review states that “experimental outcomes are amazingly different, covering all possible results: insulating, semiconducting, ohmic, and even induced semiconductivity”, and that “the conductance behavior of DNA remains poorly understood”. (Endres RG, et al. Colloquim: The Quest for High-Conductance DNA. Reviews of Modern Physics, 76, 195-214, Jan. 2004). Given this evidence, it can be concluded that the conductivity or other electrical response characteristics that DNA might exhibit in any one situation, is nowhere as predictable and straightforward as that shown by metallic radio antennas.

2. The electromagnetic response characteristics of DNA are now known to be associated with its surrounding medium. The surrounding Manning charged ion cloud is highly responsive to electromagnetic emissions. The polar water molecules are also responsive to such emissions to some degree. Therefore, drawing a complete analogy between metallic radio antennas and DNA chain molecules is inappropriate for purposes of characterizing DNA resonant responses. Certain critical electrical characteristics of DNA resonant response, and how such response is connected to dipole moment and the counterion cloud, is further discussed in section 6 below.

3. DNA is essentially a flexible linear crystalline material. A major DNA biophysics text (Yakusevich, LV, *Nonlinear Physics of DNA*. Wiley: 1998, p.13) states, “the DNA molecule has a ‘skeleton’ (sugar-phosphate chain) with an accurately repeating pattern of atoms along the chain. Due to these properties DNA is to a certain extent similar to one-dimensional periodical structure which is known in physics as quasi-one-dimensional crystals...DNA is not a rigid system, but a flexible one.” Another source (Takashima S., *Electrical Properties of Biopolymers and Membranes*. Hilger, 1989, p. 200) similarly teaches, “double helical DNA has a highly ordered internal structure with a remarkable regularity. In other words, helical DNA is in a crystalline state.” This is a crucial concept which is foundational to how DNA responds to electromagnetic emissions in a manner that is different from metallic antennas, which is not considered crystalline material.

4. Further scientific analysis of such flexible coiled and supercoiled DNA has shown that the average base pair measurement parameter (used in this patent application) does remain consistent even when the DNA molecular chain is in coiled formation. An article abstract on this subject states: “we have deduced an average structure for negatively supercoiled circular DNA in solution...the length of the superhelix axis is constant at 41% of the DNA length, whereas the superhelix radius decreases essentially hyperbolically as supercoiling increases.” (Boles TC et al, *Structure of Plectonemically Supercoiled DNA*, J Mol Biol 213, 931-951, 1990). The definition of a superhelix axis length consists of the length of the supercoiled DNA strand. In the body of the article, the authors state the average base pair spacing measurement for their chain length computation and subsequent mathematical analytical procedures: “We assume this length to be the number of base pairs in the plasmid multiplied by 3.35 angstroms per base-pair” (op. cit., p. 933). Thus we see acceptance in the scientific community that superhelix lengths are consistently dependent on the original length of the initial DNA backbone chain, and it is the radius of the coil that changes (becomes more compact) as supercoiling increases. This backbone length dependence is further illustrated in another source from the literature. In the book titled “DNA Topology and its Biological Effects” (Cozzarelli NR & Wang JC, p.169, Cold Spring Harbor Press, 1990), is a drawing with examples of plectonemic and solenoidal

supercoiled DNA models, and is captioned as follows: "In all cases, the length of the DNA is 15,500 angstroms (4.6 kb)". The division of 15,500 angstroms by 4,600 base pairs gives a result of 3.37 angstroms, which is suitably close to the 3.4 angstrom measurement used by this applicant, and which is commonly used by other writers of biophysics articles in this field. These scientific sources demonstrate that the 3.4 angstrom base pair separation measurement is a scientifically accepted and useful average measurement parameter for not only straight but also coiled forms of DNA.

5. DNA's crystalline characteristics do not necessarily require that the molecular chain be in a straight linear form in order to respond to incoming electromagnetic radiation. One of the journal articles submitted by the applicant as prior art (Edwards GS et al. Microwave-Field-Driven Acoustic Modes in DNA. *Biophys J* 47, p. 806, June 1985) explains in the appendix: "DNA molecules of several thousand base pairs are exposed to a time varying, essentially uniform field at microwave frequencies...Each base pair has two net negative charges  $q$  that experience a force from the field  $E$ . The resulting mechanical displacement is coupled into a neighboring base pair by bonded potentials...Field-induced displacements develop into a coherent mode when the frequency of excitation  $\omega/2\pi$  corresponds to an acoustic resonance, i.e., when a standing wave develops on a finite DNA molecule. Mechanical excitations can draw large amounts of power from the electromagnetic field only when the acoustic resonance condition is satisfied. This is the source of the frequency-length dependence." This teaches the mechanism by which base pairs are affected by the field, which then creates an electro-mechanical response, and which is further transferred into neighboring base pairs. A second source (Zhang C, Harmonic and subharmonic resonances of microwave absorption in DNA. *Physical Review A* 40(4), 2148, 1989) teaches: "It is well known that the permanent dipole moments of bases are considerably large...the coupling of the external electric field with these dipole moments may produce a moment force for each base. So a torsional acoustic wave propagating along the DNA chain may occur." This reinforces the concept stated by the previous author, that forces which originate in the electrical field emission will induce a mechanical response in the individual base pairs.

6. The large dipole moments of DNA helical molecules are described by Takashima as being 20 debye per each 3.4 angstrom unit (op. cit., p.202). This can produce a dipole moment in the area of 100,000 debye for a molecule of only 5,000 base pairs length. These considerable dipole moments are also reviewed by Foster [Foster KR, Thermal and Nonthermal Mechanisms of Interaction of Radio-Frequency Energy with Biological Systems. IEEE Transactions on Plasma Science 28(1), 15-22, 2000], in which he shows typical dipole moments for DNA as being in the area of 100,000 debye (variable); and that for hemoglobin and water as being respectively, 170 and 1.8 debye. Takashima also lists dipole moments of various protein molecules as being in the range of 100-1,000 debye (op. cit., p.137). With additional rigorous analysis and consideration of prior research, he further concludes that (op. cit., p.202) "we can reach a conclusion that counterion polarization theory can account for the size dependence of the dielectric increment and relaxation time of a DNA molecule. The dominant component of the dipole moment of DNA, therefore, seems to be an induced moment due to counterion fluctuation." Thus not only would reaction of the surrounding counterion cloud to the external electric field component play into the ultimate response of DNA to electromagnetic emissions, but the size of the DNA molecule will also effect the dielectric and other electrical parameters such as relaxation (response) time. This is further reinforced when Takashima states (op. cit., p.203), "clearly, the dielectric increment is proportional to the square of the effective length of DNA, an indication that helical DNA has a large longitudinal dipole moment."

7. Yet another source [Kohli M, et al, Calculated Microwave Absorption of Double-Helical B-Conformation Poly(dG)-Poly(dC). Biopolymers, 20, 853-864, 1981] states: "A gently curving segment [of DNA] could support resonant acoustic modes matched to its entire length but only have some fraction of its length properly oriented so as to absorb in a given field." Once again, here is indication that an absorption by only a portion of the DNA molecular chain may be required to initiate excitation of the entire molecule. It is further noted that this phenomenon can be incited by an electromagnetic wave of such frequency and wavelength that would couple to the DNA strand in a manner that relates to the length of its chain. The method in the current application under consideration attempts to achieve such a resonant response by giving special

attention to the electrical in-vivo parameters, thus increasing the likelihood and power of the response.

8. It is indicated by the examples in the present specification that the DNA/RNA of pathogens would be the primary target molecules for purposes of this method. Boles (op. cit., p. 948) highlights an importance difference in the DNA prokaryotic structure typical of pathogens versus that of eukaryotes, stating that "in prokaryotes, it has been estimated that 40% of the DNA is plectonemically supercoiled...but in eukaryotes, the vast majority of the DNA is solenoidally wound in nucleosomes." It is well known to those skilled in the art, that prokaryotic DNA lacks histone proteins and nucleosome coils, allowing for a more simplified morphology than that of eukaryotic DNA. Takashima also states that (op. cit., p.198) "the complexation of DNA with histone is expected to alter the charge distribution and, consequently, the value of the dipole moment...The dielectric increment of DNHi [complexed nucleohistone] is, as expected, smaller than that of DNA. This result proves that the presence of histone molecules shields the charges of DNA and decreases its dipole moment." The method originally stated in the present specification, as well as the reinforcing concepts presented in this response, would therefore indicate enhanced applicability to pathogenic prokaryotic DNA as opposed to human eukaryotic DNA due to lack of histones and larger dipole moment.

Furthermore, a 1987 research article (Sagripanti J, Swicord ML, Davis CC. Microwave Effects on Plasmid DNA. Radiation Research 110, 219-231, 1987) teaches that (p.223) "analysis of exposed DNA by AGE (agarose gel electrophoresis) showed increased amounts of relaxed circular or linear DNA after MW (microwave) exposure...the relaxation of DNA is power dependent." This would indicate the tendency for DNA to release its coiling tendencies when under the influence of electromagnetic fields, and to be enhanced when they are frequency-specific due to the mechanical effects of the field on the outer charged phosphate groups and the counterion cloud. The authors also state that (op. cit., p.219) "physical studies carried out in our laboratory have shown MW absorption by DNA molecules in aqueous solution. The microwave absorption was dependent upon the size of the DNA molecule." These facts, when coupled with the important indication that only a fraction of the chain length may need to be properly oriented



to the field in order to achieve excitational resonance throughout the entire span of the molecule (as reviewed in section 7), again asks that the entire DNA resonance phenomenon be viewed in a very different light from that of metallic radio antennas.

9. Yakusevich (op. cit., p.6 ff) further elaborates that there are elaborate interactions among the sub-molecules and atoms of the DNA chain which stabilize its secondary structure (such structure includes the diameter of the chain, the base pair spacing, rotation of the bases, length of the full turn, etc). These include specific bond and energy forces which hold the atoms in the positions characteristic of a crystalline material. While the bonds may stretch or contract slightly, exceeding the capacity of the bond lengths and interatomic forces would cause the failure and destruction of the molecule. It is only logical that in spite of the presence of coiling and supercoiling, the bonds and energies must remain within fairly strict parameters to keep the overall molecular structure intact. The 3.4 angstrom spacing measurement reflects this fact, because it is repeatedly stated in the literature to be an *average* spacing parameter through the length of a DNA chain. Furthermore, it is noted that bends and coils seen in DNA exist in an electron microscope visual frame of reference; this is in contrast to the miniscule adjustment of bond lengths and energies that may occur in order to achieve bending and coiling, which is on a scale of measurement 3-5 orders of magnitude smaller than the macroscopic parameters of such bends and coils. This would produce only a minute variation in any one base pair spacing measurement (so as to avoid rupturing the bond), and even then would be distributed only over a limited length of base pairs in the chain.

The Office Action from 9-9-04 also notes (page 3, bottom), “applicant then argues that the complexity of genomic material in a living cell is merely addressed by multiplying the base pair number by the average spacing between base pairs. Again this allegation ignores the factual basis for this rejection that the base pairs in the genomic material in a living cell is not additively lined up to result in a length such as a linear antenna for receiving electromagnetic energy.”

The applicant respectfully maintains that based on evidence from the aforementioned scientific sources, the receiving DNA molecule does not need to be linear in order to respond to

electromagnetically induced excitation; and that similar to a piece of heavy rope, and because of its crystalline structure, when a theoretically straight piece of DNA becomes curved it will maintain the same internal structure and thus overall length parameter as when it was straight. The scientific literature in its experiments and analysis, supports consistent use of the 3.4 angstrom average measurement over the length of a DNA molecule, whether it is straight or curved. The objections of the office regarding use of the 3.4 angstrom measurement for the purposes of the method in this application, are therefore respectfully traversed.

The applicant also calls attention to a basic process and phenomenon shown in articles previously submitted as prior art. This would include Edwards GS et al 1984, and Swicord ML 1983, in which an electromagnetic emission produces a resonant response which relates to the length of the DNA chain. The resonant response in those seminal research articles was initially characterized acoustic and longitudinal in nature, along the length of the chain. Other scientists have performed additional research and analysis which builds on those early experimental results, the body of which is too large to give complete attention to in this response. The applicant cites however, two additional papers. The first (Van Zandt LL, Resonant Microwave Absorption by Dissolved DNA, Physical Review Letters 57(16), 2085, 1986) states in the abstract: "The anomalous microwave absorption resonances recently observed in aqueous solutions of DNA are explained in terms of a layered structure of water molecules around the polymer. At high frequencies the interactions with water become elastic instead of viscous." This reinforces the fact that the DNA resonances described by the author are caused in part by, and interact with, the medium surrounding the molecule. And in the body of the article, he states, "the frequency locations of the resonances are close to those expected for "organ pipe" modes of the polymer, longitudinal compressional standing waves." This statement constitutes a direct connection with molecule length. A later article by the same author (Van Zandt LL, Why Structured Water Causes Sharp Absorption by DNA at Microwave Frequencies, Journal of Biomolecular Structure & Dynamics 4(4), 569-582, 1987), not only affirms that "the base pairs are separated by 3.4 angstroms", but adds (op. cit., p.570) that "a cloud of counterions, almost exclusively cations at a close range, surrounds the chain. Overall charge neutrality is achieved at as short a range as 5 to 10 angstroms out from the polymer radius. Within the neutralization, the

highly polar water molecules are subject to strong electric fields. The water becomes highly structured and layered.” This material again demonstrates the highly specialized environment around the immediate area of the DNA molecule, and that such an environment does contribute an important role in the electronic resonant excitation associated with the molecule. This is affirmed with another statement made after rigorous analysis (op. cit. p.577), that “on a length of helix L many harmonics of differing wavelengths could propagate.” This lends yet more weight to the importance of molecule length in the resonant response. And in another coherent description of the process, this same biophysicist states (Van Zandt LL & Davis ME, Theory of the Anomalous Resonant Absorption of DNA at Microwave Frequencies, Journal of Biomolecular Structure & Dynamics 3(4), 1045-1053, 1986) that “the solvent is electrically active and so responds to the electric fields, both DC and microwave, in the molecule vicinity...the presence of the charged ions in the water provides a means whereby the electric field can interact directly with the solvent in addition to the indirect effect of first driving the molecule that subsequently mechanically couples to the liquid.” It can be seen therefore that the electric field effects of the electromagnetic wave not only can drive the highly-charged base pairs into mechanical oscillation, but that the response of the surrounding solvent may be likewise coupled to that excitation.

In view of these mechanisms, the applicant maintains that electromagnetic emissions as calculated in the method under consideration, can excite a resonant response in DNA that involves not only the molecule itself, but the surrounding water and ion cloud as well. These additional factors are what makes the response of a DNA molecule very different from those associated with a metallic antenna used in radio technology, as described in the objections from this office. While the ultimate equation used by the applicant is similar to the velocity – frequency – wavelength equation so often used in radio and other resonance-related sciences, we must remember that the velocity factor is determined in part by the electrical permittivity, and that the electrical permittivity is influenced by the mechanisms previously described in this response, including (but not necessarily limited to) the dipole moment of the molecule, which is itself influenced by its length and the surrounding medium. The fact that this method is eliciting positive clinical responses along with repeatability, that it shows specificity and selectivity of

frequencies, and is backed by supportive theory from the scientific literature, allows this method to be characterized as predictive of usefulness against pathogens with a high enough rate of efficacy to warrant further research and clinical use. The applicant therefore respectfully traverses this office's objections which are based on technical antenna and wavelength matters as described in its previous communications from March and September 2004, the concepts from which, according to the examiner's statements, implied lack of enablement per 35 U.S.C. § 112, first paragraph.

### **Resonance**

The applicant acknowledges conflict and confusion arising from a statement made in her previous response dated June 9, 2004 regarding the matter of resonance. The statement in question begins at the bottom of page 17 of that document and reads: "Applicant respectfully submits that, based on numerous field demonstrations, a frequency-emitting device programmed with frequencies determined according to the claimed methods selectively influence a target genomic material in a desired manner (whether or not "resonance" of the genomic material is achieved)." Applicant reiterates that this material was submitted by her past counsel to this office, without opportunity of approval before it was sent. Applicant maintains that the above statement is causing considerable confusion, has additionally caused the office to misunderstand the intent of the resonance matter, and therefore asks that the statement be stricken from consideration. Applicant further asks that the following comments be now taken under consideration regarding the matter of resonance.

The definition and phenomenon of resonance, as reviewed by the examiner in the recent phone interview, does indeed include a mechanism of energy transfer via matching of some physical parameter. In the method under consideration, a tool is offered to match the wavelength of an electromagnetic wave in a harmonic manner to a physical parameter, than being the length of a pathogenic genomic chain molecule.

To successfully achieve a desired resonant event, however, would also require delivery of the appropriate matching wavelength (and thus frequency) at an optimal power level. The

required power level used would be determined by what level of resonant outcome was desired. An analogy may be seen from the often-compared resonance of a crystalline wineglass. A low-power delivery of the appropriate wavelength or frequency would indeed resonate the glass, making it ring, but not necessarily shatter it. A higher-powered delivery would also resonate the glass, and may indeed shatter it. In both instances, it will be noted that some type of resonant event did occur.

In the instance of using this method to resonantly excite a genomic molecule, it would be difficult (without use of extremely specialized equipment, that is), to immediately observe any resonant response in the molecule under consideration. And it would be also difficult to immediately ascertain a resonant event of the molecule itself, under in-vivo conditions. Nonetheless, a resonant event or phenomenon may have occurred. Without undue and lengthy experimentation, the best way to determine if a resonant event occurred in vivo, is via appropriate lab testing and/or positive clinical outcomes.

The applicant therefore asks that due consideration be given to the use of the word “resonant” as a descriptive adjective, which logically relates the usual concepts of resonance in the physics literature to the DNA resonance phenomena described in the biophysics literature reviewed above, as well as to the ultimate clinical results that are occurring in the use of this method. The applicant maintains that given the totality of clinical results, the close relationship of the method under consideration to general resonance phenomena, and the prior material presented in the DNA-related biophysics literature, that resonance is likely to be occurring with use of this method.

The applicant also points out that the phenomenon of a resonant event is not necessarily dependent on the use of an extremely exact frequency. The condition necessary for resonant energy transfer when diagrammed on a chart, resembles a bell curve. It is possible that in some circumstances, a resonant event may also occur near the optimum natural frequency of a system, and still achieve a desired outcome. This concept is further clarified from a physics source (Hecht E. Physics, Vol. 1, p.416. Brooks/Cole Pub. Co., 1994): [as the emitted frequency] “approaches the natural frequency of the system, the resulting oscillation will dramatically

increase in amplitude. The vibrational amplitude will reach a maximum when  $f = f_{\text{subscript } 0}$ , a condition known as resonance.” And as previously mentioned, the ultimate success of the desired resonant event, whether at the optimum frequency or a nearby frequency, may also depend on the power level, waveform, and other characteristics of frequency delivery.

The applicant thus maintains that while the method under consideration offers the best possible determination of frequency, which is the primary factor that will enhance occurrence of a resonant event, other factors outside of the realm of this method could also influence the ultimate success of the desired resonant outcome. In that sense and only in that sense, the actual desired resonant event for genomic material (as opposed to occurrence of resonance to varying degrees) may or may not be immediately seen at a macroscopic laboratory or clinical outcome level of observation, because the user may not have included optimal power level, etc. in the delivery protocol.

The applicant further notes that in the patent (US 6,060,293) previously addressed in this response, the concept of a specific type of molecular chain resonance is allowed, even though the event was not immediately observable and needed further testing to establish certainty; and asks therefore that this applicant be likewise allowed use of the concept of resonance, albeit in a different manner (applicant addresses longitudinal mode as opposed to the torsional resonant mode used in the aforementioned patent).

The applicant respectfully requests that with consideration of the foregoing comments, that the objections from the office regarding resonance be withdrawn.

## **CONCLUSION**

The applicant maintains the communication from June 9 2004, in that the specification describes the subject matter in such a way as to enable one skilled in the art to make and/or use the invention, as set forth in claims 1, 15, 17, and 28. Such a person would be enabled to make and/or use the invention within the scope of those claims. Claims 2, 4-14, 16, 18-27, and 29 depend from claims 1, 15, 17, and 28, and are thus also enabled by the specification.

Applicant states that a full and complete response has been made herein to the past two Official Actions dated March 9 and September 9 2004, and as such, all pending claims in this application are now in condition for allowance. The applicant respectfully requests early consideration of the present application, entry of the amendment to claim 5 previously agreed to, withdrawal of all rejections, and allowance of all pending claims.

Respectfully submitted,

*Charlene A. Boehm*

*January 7, 2005*

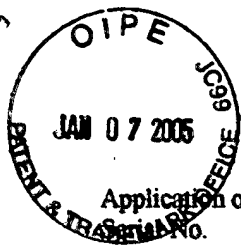
Charlene A. Boehm

January 7, 2005

Charlene Boehm  
320 Gilbert Rd.  
Columbus, NC 28722  
(828) 863-4317







Application of : Charlene Boehm  
Serial No. : 09/780,901  
Filed: : February 9, 2001  
For : Methods for Determining Therapeutic Resonant Frequencies  
Examiner : Ardin H. Marschel  
Art Unit : 1631

---

The enclosed document and references are attached to the applicant's response dated January 7, 2005.

**CB**

---

**From:** "Boggs, Mike" <MBoggs@KilpatrickStockton.com>  
**To:** <soundtree@alltel.net>  
**Sent:** Wednesday, June 09, 2004 1:05 PM  
**Attach:** Boehm Therapeutic Resonant Frequencies 1.111 Amendment & Response to 3 9 04 Office Action(v1).DOC  
**Subject:** Response to Office Action

Dear Charlene,

Please find attached a copy of my draft response to the Office Action in your patent application. I plan to discuss with Charles this afternoon, and to file the response by 5:00 today. If you have a chance to review, please notice in particular the Interview Summary beginning on p. 11 and the section related to enablement beginning on p. 14.

If you have any questions or further thoughts, please let me know. I will send you a copy of the response as filed.

Thanks for your input in this process - it is valuable.

Best regards,

Mike Boggs  
Kilpatrick Stockton LLP  
1001 West Fourth Street  
Winston-Salem, NC 27101-2400  
(336) 747-7536 (Direct Dial)  
(336) 734-2632 (Fax)  
[MBoggs@KilpatrickStockton.com](mailto:MBoggs@KilpatrickStockton.com)

Confidentiality Notice: This communication constitutes an electronic communication within the meaning of the Electronic Communications Privacy Act, 18 USC Section 2510, and its disclosure is strictly limited to the recipient intended by the sender of this message. This transmission, and any attachments, may contain confidential attorney-client privileged information and attorney work product. If you are not the intended recipient, any disclosure, copying, distribution, or use of any of the information contained in or attached to this transmission is **STRICTLY PROHIBITED**. Please contact us immediately by return e-mail or at (336) 607-7300, and destroy the original transmission and its attachments without reading or saving in any manner.

<<Boehm Therapeutic Resonant Frequencies 1.111 Amendment & Response to 3 9 04 Office Action(v1).DOC>>

1/7/05

## Colloquium: The quest for high-conductance DNA

R. G. Endres

*Center for Computational Sciences and Computer Science & Mathematics Division, Oak Ridge National Laboratory, Oak Ridge, Tennessee 37831-6114, USA*

D. L. Cox and R. R. P. Singh

*Department of Physics and Center for Biophotonics Science and Technology, University of California, Davis, California 95616, USA*

(Published 12 January 2004)

The DNA molecule, well known from biology for containing the genetic code of all living species, has recently caught the attention of chemists and physicists. A major reason for this interest is DNA's potential use in nanoelectronic devices, both as a template for assembling nanocircuits and as an element of such circuits. Without question, a truly conducting form of DNA would have a major impact on developments in nanotechnology. It has also been suggested that extended electronic states of DNA could play an important role in biology, e.g., through the processes of DNA damage sensing or repair or through long-range charge transfer. However, the electronic properties of DNA remain very controversial. Charge-transfer reactions and conductivity measurements show a large variety of possible electronic behavior, ranging from Anderson and band-gap insulators to effective molecular wires and induced superconductors. Indeed, understanding the conductance of a complicated polyelectrolytic aperiodic system is by itself a major scientific problem. In this Colloquium, the authors summarize the wide-ranging experimental and theoretical results and look for any consistencies between them. They also pose simple questions regarding the electronic states of DNA within the framework of generalized Hückel and Slater-Koster theories. The Colloquium provides a quantitative overview of DNA's electronic states as obtained from density-functional theory, focusing on dependence on structure, on molecular stretching and twisting, and on water and counterions. While there is no clear theoretical basis for truly metallic DNA, situations are discussed in which very small energy gaps might arise in the overall DNA/water/counterion complex, leading to thermally activated conduction at room temperature.

### CONTENTS

|  |     |
|--|-----|
| I. Introduction  | 195 |
| A. Why think of DNA as an electronic material?           | 195 |
| B. DNA: A molecular wire in biological systems?          | 197 |
| C. DNA: A building block in molecular electronics?       | 197 |
| D. Overview of this Colloquium                           | 198 |
| II. Basic Concepts                                       | 198 |
| A. The $\pi$ - $\pi$ electronic coupling                 | 198 |
| B. Coupling to vibrations                                | 199 |
| III. Experimental Overview                               | 200 |
| A. Charge transfer                                       | 200 |
| B. Conductivity  | 200 |
| IV. Theoretical Efforts                                  | 205 |
| V. The Role of Structure and Environment in Conductivity | 207 |
| A. Effects of DNA structure on $\pi$ coupling            | 207 |
| B. Impurity states and doping                            | 209 |
| VI. Conclusion   | 212 |
| Acknowledgments  | 212 |
| References   | 212 |

### I. INTRODUCTION

Half a century after the discovery of the DNA structure as reported by Watson and Crick (1953), celebrations of this important molecule abound. The principal story of DNA has long centered on the fundamental role

this molecule plays in carrying the genetic code of organisms. However, there has been an upwelling of recent interest in its electronic properties, motivated by both biological and technological concerns. The highly specific binding between single strands of DNA, its related self-assembly property, and the ability to synthesize DNA in whatever sequence you want (versus the hit and miss control over, say, carbon nanotubes) have made it a suitable candidate for use in molecular electronics. Motivated by these potential applications, numerous studies of charge transport in DNA have been carried out. However, although some consensus on the dominant mechanisms of single-electron transfer in DNA seems to be emerging [see the recent review by Dekker and Ratner (2001)], the nature of DNA's intrinsic conductance properties remains highly controversial.

#### A. Why think of DNA as an electronic material?

As early as 1962, Eley and Spivey suggested that the interbase hybridization of  $\pi_z$  orbitals perpendicular to the planes of the stacked base pairs in double-stranded DNA [with the DNA helical axis parallel to the  $z$  coordinate axis, as in Fig. 1(a)] could lead to conducting behavior (Eley and Spivey, 1962). There are similar stacked aromatic crystals that are indeed metallic (Roth, 1995). The most famous of such materials are the Bechgaard salts, e.g.,  $(\text{TMTSF})_2\text{PF}_6$  (Fig. 2). How-

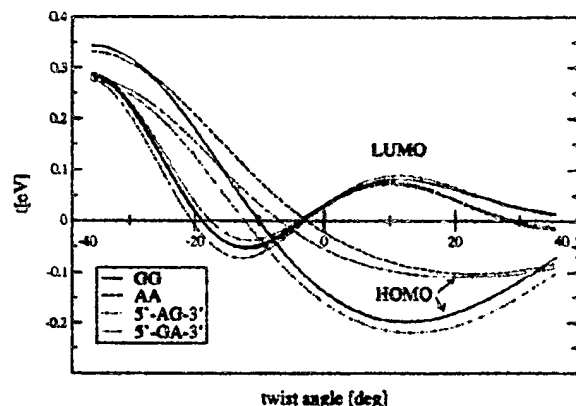


FIG. 4. Change of electronic coupling  $t$  between frontier orbitals (HOMO's and LUMO's) of two base pairs with a relative twist angle about the equilibrium angle  $36^\circ$  (set to zero). The base pair separation is kept fixed at  $z=3.4 \text{ \AA}$ . The different plots correspond to various base pair dimers (two-base-pair-long DNA), e.g., sequences GG, AA, AG, GA counted from the 5' end to the 3' end.

ergy corresponding to the electron affinity energy) between different base pair dimers. The coupling between HOMO's is important for hole transport, while the coupling between LUMO's is important for electron transport.

According to Fig. 4 there are sign changes of  $t^{n,m}$  as a function of the twist angle. Interestingly, the sign changes occur near the equilibrium twist angle of A-DNA. The LCAO coefficients stay approximately constant during the rotation, so that the sign changes must stem from the interaction matrix elements  $V_{ij}^{12}$ , which depend strongly on the geometry of the base pair dimer. At ambient temperatures, the twist angle has a standard deviation of about  $8^\circ$  (Young *et al.*, 1997). In the interval  $(-8^\circ; +8^\circ)$  it is possible that  $t^{n,m}$  vanishes. One can easily imagine that base pair to base pair charge transport is limited by the low twisting frequencies, of order  $10^{11}$ – $10^{12}$  Hz, particularly in structures close to the A form. Separately at an angle of  $-36^\circ$ , the base pairs are perfectly aligned (for identical base pairs) and parallel to each other. This leads to optimal  $\sigma$  overlap and to a maximal  $t^{n,m}$ . At least for identical base pairs this can easily be rationalized, since we get approximately  $t \sim \sum_i^N V_{ii}(c_i)^2 > 0$ , where  $V_{ii}$  are all positive due to  $\sigma$  overlap and add up to give a large contribution. [Note that  $V_{ij}$  with  $i \neq j$  are typically very small; note also that for simplicity we have omitted here the superscripts to the coefficients  $c_i$  that appear in Eq. (4).]

The dependence of  $t^{n,m}$  on the base pair separation is less dramatic and is discussed elsewhere (Endres *et al.*, 2002).

### III. EXPERIMENTAL OVERVIEW

#### A. Charge transfer

Hole transfer reactions in DNA have been studied by Henderson *et al.* (1999), Lewis *et al.* (2000), Giese *et al.*

(2001), and others. Initially, DNA is doped (in chemical terminology, oxidized or reduced). The base guanine is an easy target for many oxidizing agents. A hole placed in a guanine's HOMO is only about 0.2 eV above the next lower occupied orbitals (of adenine; thymine and cytosine are even lower; Bixon and Jortner, 2001a) and can begin to migrate through the DNA to find other easily oxidizable sites, like other guanines or sequences of guanines. In this scenario of hole transport DNA's LUMO is not involved, because it is about 4 eV higher in energy. The charge-migration mechanism can involve a single quantum-mechanical tunneling event at short distances, a phenomenon first described quantitatively by the celebrated theory of Marcus (1956a, 1956b, 1993, 1998). Alternatively, charge transfer can involve several direction-uncorrelated tunneling events displaying a one-dimensional random walk. A more detailed introduction to the theory of charge transfer is given in Sec. IV. Put simply, the picture that emerges from experiments (Dekker and Ratner, 2001) is that superexchange (tunneling) occurs between guanines (or guanine dimers and trimers) separated by three or fewer A-T base pairs, while for larger separations diffusive hopping dominates the transfer. Some of the pioneering work by Barton, Zewail, Wan, and co-workers on photoinduced charge transfer shows a weak distance dependence (Murphy *et al.*, 1993; Wan *et al.*, 1999), which led to suggestions that DNA could act as a "molecular wire." However, later work using different donors and acceptors argued against the wirelike picture for DNA (Wan *et al.*, 2000). (We note that the use of the term "wire" in the DNA charge-transfer literature is somewhat problematic, if not wholly ill defined. In this context we take "wire" to mean that injected holes or electrons can enjoy long-range transport, i.e., over tens of angstroms, on fast time scales of picoseconds or less.) The interpretation of some of these experiments may be even more uncertain, since it is not even clear if the reaction involves electron or hole transfer.

#### B. Conductivity

The question of whether DNA is intrinsically conducting is an unsolved problem. The experimental outcomes are amazingly different, covering all possible results: insulating (Braun *et al.*, 1998; de Pablo *et al.*, 2000; Storm *et al.*, 2001; Zhang *et al.*, 2002), semiconducting (Porath *et al.*, 2000), Ohmic (Fink and Schönenberger, 1999; Cai *et al.*, 2000; Tran *et al.*, 2000; Rakin *et al.*, 2001; Yoo *et al.*, 2001), and even induced superconductivity (Kasumov *et al.*, 2001). One difficulty is to make cleanly reproducible and easily interpreted experiments with nanoscale dimensions. The other difficulties have to do with the large number of "variables" (experimental conditions) on which the outcome of the experiments depend. Furthermore, experimental results are often presented in short-format letter journals condensing the description of experimental conditions and protocols. This makes it hard for one to judge the quality of the experi-

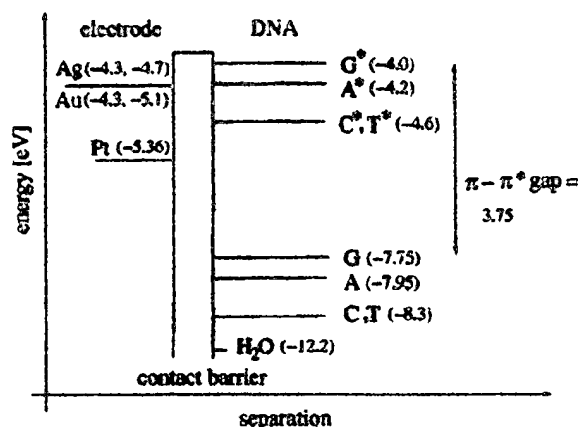


FIG. 5. Schematics of metal work functions and DNA energy levels at an electrode/DNA junction. The values of the metal work functions and the first ionization potential of gaseous water are taken from Hodgman and Veazey (1966), Ashcroft and Mermin (1976), the website <http://kasap3.usask.ca/server/kasap/Tables/Metal1.html>, and Barrow (1988). The value of water is expected to change drastically in the proximity of charged DNA and counterions. The DNA gap of 3.75 eV is taken from an optical absorption measurement, which also corresponds to the excitation energies of single bases (Helgren *et al.*, 2002). The excited-state energies of the bases are obtained from the single-base ionization energies by simply adding the gap size. The ionization energies are a tricky business: according to Koopmans's theorem the ionization energies correspond to the HOMO energies obtained from a Hartree-Fock *ab initio* method. The guanine (G) value is taken from Sugiyama and Saito (1996) and Wetmore *et al.* (2000), which is close to the experimental value of guanine in the gas phase (Orlov *et al.*, 1976; Lias *et al.*, 1988). The values for adenine (A), thymine (T), and cytosine (C) are not taken from an *ab initio* calculation or experiment of single bases, since they may be too negative relative to G in a DNA environment. From analyzing yield data of charge transfer in DNA (Bixon and Jortner, 2001a), they are likely to be closer to G than isolated bases in the gas phase (Orlov *et al.*, 1976; Lias *et al.*, 1988) or solution (Seidel *et al.*, 1996; Steenken and Jovanovic, 1997).

ments and relate them to one another. Of course, in this Colloquium we can only comment upon the details presented in the literature.

Assuming that the literature data are not artifacts and provide useful information about DNA conductivity, we can separate the sources of experimental uncertainties into two categories:

- **Contacts between the electrode and the DNA molecule:** The contact is characterized by the work function of the electrode, as well as the nature of the tunneling barrier. Is there direct metal- $\pi$  orbital contact or do charge carriers first have to tunnel through the backbone? If so, what is the size of the barrier? Unfortunately, only the work functions of metal electrodes are more or less known. In the important case of gold, it is not even clear if the Au work function is below or above the DNA LUMO (Fig. 5). [Electron affinity

measurements of single bases in the gas phase suggest that the Au work function is below (Afsharouni *et al.*, 1998).]

- **Differences in the DNA molecules and their environments:**

There are many factors that influence DNA conductivity:

- (1) DNA sequence. Figure 5 shows estimates of metal work functions and ionization potentials of bases. Since each base has its own molecular energy level, a nonperiodic sequence will lead to disorder along the one-dimensional molecule.
- (2) Length of the DNA molecule.
- (3) Character of the DNA molecule (e.g., ropes vs single molecules).
- (4) Environment of DNA (influence of water and counterions). Here, for example, the number of water molecules is critical in influencing structure: for five to ten water molecules per base the A-DNA structure obtains, while for >13 water molecules per base the B structure is preferred (Warman *et al.*, 1996).
- (5) Microstructure of DNA (dependent upon humidity, stretching, or combing preparation conditions).
- (6) Interfacial character (e.g., free-standing molecules, surface-bound DNA on, say, mica).
- (7) Preparation and detection protocols [drying of DNA via flowing  $N_2$  gas, which tends to provide two to three water molecules per nucleotide (Tran *et al.*, 2000); detection of single molecules by scanning probe microscopies or electron microscopies, which can "dope" the molecules].

Some of the above-mentioned variables are hard to control, e.g., the nature of the contact and the actual structure of DNA. Some success has recently been achieved by Hartzell *et al.* (2003a, 2003b) concerning the dependence of the conductivity on the nature of the contact to the electrode as well as on whether DNA is nicked or repaired. However, the same authors admit that, while some experimental parameters are rather well controlled, other important ones, like how many DNA molecules are actually bridging the electrodes, are not.

A key experimental challenge in measuring DNA conductance lies in the attachment of a DNA bundle or single molecule to two electrodes. This has been made possible largely due to advancements in nanotechnology. Electron-beam lithography is used to fabricate nanoelectrodes, atomic force microscopy (AFM) and low-energy electron point source (LEEPS) microscopy are used to image the sample, and scanning tunneling microscopes (STM) can be utilized to induce a tunneling current. In order to attach single DNA molecules to metal electrodes, a DNA oligomer-based<sup>1</sup> "gluing" technique

<sup>1</sup>An oligomer is a molecule comprising only a few base pair monomers.

pendent of the base pair sequence and could allow for extended Bloch states. Nevertheless, conduction through the backbone remains questionable because of the insulating sugars separating phosphate groups from each other.

Clearly more studies will have to be done in order to obtain a reliable picture, since DFT calculations on systems containing ions with long-range Coulomb interactions are still quite challenging. Another question one must ask is: How well can potential solvent/backbone-impurity states of wet/dry DNA support actual transport?

## VI. CONCLUSION

In this Colloquium we have presented an elementary introduction to the electronic properties of DNA. We began by discussing its similarities to certain charge-transfer molecular metals. We then summarized recent experimental and theoretical studies of electron transport in DNA. For migration of a single hole in DNA, a general theoretical consensus appears to be emerging. However, the conductance behavior of DNA remains poorly understood. Nevertheless, insights from *ab initio* methods do help explain some of the conflicting experimental outcomes. It appears that drying DNA—as is usually done prior to measuring the conductance—can lead to DNA conformations with localized electronic  $\pi$  states, although hole doping of the backbone by counterions might be possible. On the other hand, wet DNA may support electrical current, partly due to solvent impurity states sitting in the large  $\pi$ - $\pi^*$  energy gap. In the case of divalent magnesium counterions, these might even electron-dope unoccupied  $\pi^*$  states.

Whether the “molecule of life” can also lead us into a second industrial revolution cannot yet be said. We are just at the beginning. The first DNA field-effect transistor has been built (Yoo *et al.*, 2001), and more DNA-based molecular electronic devices will likely follow.

## ACKNOWLEDGMENTS

We would like to thank E. Artacho, P. Ordejón, D. Sánchez-Portal, and J. M. Soler for providing us with their *ab initio* code SIESTA. R.G.E. thanks R. Laughlin for providing temporary work space at Stanford University, where part of the writing was done. This work was supported by the U.S. Department of Energy, Office of Basic Energy Sciences, Division of Materials Research, and in the latter stages by the Center for Biophotonics, an NSF Science and Technology Center, managed by the University of California, Davis, under Cooperative Agreement No. PHY 0120999. This work was initiated with the assistance of a Seed Grant from the Materials Research Institute of Lawrence Livermore National Laboratories, and we acknowledge the use of the LLNL computer clusters in connection with this grant. At ORNL, R.G.E. acknowledges the support of DOE-OS through OASCR-MICS under Contract No. DE-AC05-00OR22725 with UT-Battelle LLC.

## REFERENCES

- Aflatooni, K., G. A. Gallup, and P. D. Burrow, 1998, *J. Phys. Chem. A* **102**, 6205.
- Alexandre, S. S., E. Artacho, J. M. Soler, and H. Chacham, 2003, *Phys. Rev. Lett.* **91**, 108105.
- Allemand, J. F., D. Bensimon, L. Jullien, A. Bensimon, and V. Croquette, 1997, *Biophys. J.* **73**, 2064.
- Anderson, P. W., 1958, *Phys. Rev.* **109**, 1492.
- Arnott, S., and D. W. L. Hukins, 1972, *Biochem. Biophys. Res. Commun.* **47**, 1504.
- Artacho, E., D. Sánchez-Portal, P. Ordejón, A. Garcia, and J. M. Soler, 1999, *Phys. Status Solidi B* **215**, 809.
- Ashcroft, N. W., and N. D. Mermin, 1976, *Solid State Physics* (Saunders College Publishing, Philadelphia), p. 364.
- Bakkinst, C. J., and M. B. Kastan, 2003, *Nature (London)* **421**, 499.
- Barnett, R. N., C. L. Cleveland, A. Joy, U. Landman, and G. B. Schuster, 2001, *Science* **294**, 567.
- Barrow, G. M., 1988, *Physical Chemistry*, 5th ed. (McGraw-Hill, New York), pp. 581–582.
- Basko, D. M., and E. M. Conwell, 2002, *Phys. Rev. Lett.* **88**, 098102.
- Bensimon, D., A. J. Simon, V. Croquette, and A. Bensimon, 1995, *Phys. Rev. Lett.* **74**, 4754.
- Bertin, Y. A., A. L. Burin, and M. A. Ratner, 2000, *Superlattices Microstruct.* **28**, 241.
- Bixon, M., and J. Jortner, 1999, *Adv. Chem. Phys.* **106**, 35.
- Bixon, M., and J. Jortner, 2000, *J. Phys. Chem. B* **104**, 3906.
- Bixon, M., and J. Jortner, 2001a, *J. Am. Chem. Soc.* **123**, 12556.
- Bixon, M., and J. Jortner, 2001b, *J. Phys. Chem. A* **105**, 10322.
- Braun, E., Y. Eichen, U. Sivan, and G. Ben-Yoseph, 1998, *Nature (London)* **391**, 775.
- Brauns, E. B., M. L. Madaras, R. S. Coleman, C. J. Murphy, and M. A. Berg, 1999, *J. Am. Chem. Soc.* **121**, 11644.
- Breslauer, K. J., R. Frank, H. Blöcker, and L. A. Marky, 1986, *Proc. Natl. Acad. Sci. U.S.A.* **83**, 3746.
- Briman, M., N. P. Armitage, E. Helgren, and G. Grüner, 2003, e-print cond-mat/0303240.
- Bruinsma, R., G. Grüner, M. R. D'Orsogna, and J. Rudnick, 2000, *Phys. Rev. Lett.* **85**, 4393.
- Bustamante, C., S. B. Smith, J. Liphardt, and D. Smith, 2000, *Curr. Opin. Struct. Biol.* **10**, 279.
- Cai, L., H. Tabata, and T. Kawai, 2000, *Appl. Phys. Lett.* **77**, 3105.
- Cai, L., H. Tabata, and T. Kawai, 2001, *Nanotechnology* **12**, 211.
- Carpena, P., P. Bernaola-Galván, P. Ch. Ivanov, and H. E. Stanley, 2002, *Nature (London)* **418**, 955.
- Chandrasekaran, R., and S. Arnott, 1996, *J. Biomol. Struct. Dyn.* **13**, 1015.
- Chen, J., and N. C. Seeman, 1991, *Nature (London)* **350**, 631.
- Cizek, J., A. Martinez, and J. Ladik, 2003, *THEOCHEM.* **626**, 77.
- Cocco, S., and R. Monasson, 2000, *J. Chem. Phys.* **112**, 10017.
- Conwell, E. M., and S. V. Rakhmanova, 2000, *Proc. Natl. Acad. Sci. U.S.A.* **97**, 4557.
- Cuniberti, G., L. Craco, D. Porath, and C. Dekker, 2002, *Phys. Rev. B* **65**, 241314(R).
- Dandliker, P. J., R. E. Holmlin, and J. K. Barton, 1997, *Science* **275**, 1465.
- Dekker, C., and M. A. Ratner, 2001, *Phys. World* **14** (8), 29.

---

WILEY SERIES IN NONLINEAR SCIENCE

---

*Series Editors:*

ALI H. NAYFEH, Virginia Tech

ARUN V. HOLDEN, University of Leeds

Yakushevich

NONLINEAR PHYSICS OF DNA

Abdullaev

THEORY OF SOLITONS IN  
INHOMOGENEOUS MEDIA

Nayfeh

METHOD OF NORMAL FORMS

Nayfeh and Balachandran

NONLINEAR DYNAMICS:  
CONCEPTS AND APPLICATIONS

Nayfeh and Pai

LINEAR AND NONLINEAR  
STRUCTURAL MECHANICS

Rozhdestvensky

MATCHED ASYMPTOTICS OF  
LIFTING FLOWS

---

NONLINEAR PHYSICS  
OF DNA

---

Ludmila Vladimirovna Yakushevich

*Institute of Cell Biophysics of the Russian Academy of Sciences,  
Pushchino, Russia*

JOHN WILEY & SONS

Chichester · New York · Weinheim · Brisbane · Singapore · Toronto

Copyright © 1998 John Wiley & Sons Ltd,  
Baffins Lane, Chichester,  
West Sussex PO19 1UD, England

National 01243 779777  
International (+44) 1243 779777  
e-mail (for orders and customer service enquiries) cs-books@wiley.co.uk  
Visit our Home Page on <http://www.wiley.co.uk>  
or <http://www.wiley.com>

All Rights Reserved. No part of this publication may be reproduced, stored in a retrieval system, or transmitted, in any form or by any means, electronic, mechanical, photocopying, recording, scanning or otherwise, except under the terms of the Copyright Designs and Patents Act 1988 or under the terms of a licence issued by the Copyright Licensing Agency, 90 Tottenham Court Road, London W1P 9HE, UK, without the permission in writing of the Publisher.

#### *Other Wiley Editorial Offices*

John Wiley & Sons, Inc., 605 Third Avenue,  
New York, NY 10158-0012, USA

WILEY-VCH Verlag GmbH, Pappelallee 3,  
D-69469 Weinheim, Germany

Jacarana Wiley Ltd, 33 Park Road, Milton,  
Queensland 4064, Australia

John Wiley & Sons (Asia) Pte Ltd, Clementi Loop #02-01,  
Jin Xing Distripark, Singapore 129809

John Wiley & Sons (Canada) Ltd, 22 Worcester Road,  
Rexdale, Ontario M9W 1L1, Canada

#### *Library of Congress Cataloging-in-Publication Data*

Iakushevich, L. V. (Ljudmila Vladimirovna)  
Nonlinear physics of DNA / Ludmila Vladimirovna Yakushevich.  
p. cm. — (Wiley series in nonlinear science)  
Includes bibliographical references and index.  
ISBN 0-471-97824-8 (hc : alk. paper)  
1. DNA—Structure. 2. DNA—Conformation. 3. Nonlinear mechanics.  
4. Biophysics. I. Title. II. Series.  
QP624.5.S78125 1998  
572.8'633—dc21

97-29529  
CIP

#### *British Library Cataloguing in Publication Data*

A catalogue record for this book is available from the British Library

ISBN 0 471 97824 8

Typeset in 10/12pt Times by Thomson Press (India) Ltd., New Delhi, India  
Printed and bound in Great Britain by Biddles Ltd, Guildford, Surrey  
This book is printed on acid-free paper responsibly manufactured from sustainable forestry.

## DEDICATION

The author dedicates this  
book to the memory of the  
pioneer in nonlinear  
biophysics, Professor Alexan-  
der Sergeevich Davydov



### 1.3 FORCES STABILIZING SECONDARY DNA STRUCTURE

To understand physical properties of the DNA molecule it is very important to have a clear idea about distribution of the interactions between the main atomic groups. The most important of them are those stabilizing the secondary DNA structure: the so-called horizontal or hydrogen interactions between bases in pairs, vertical or stacking interactions between neighbour bases along the DNA axis, and long-range intra- and inter-backbone forces.

#### 1.3.1 Hydrogen Interactions

In general, hydrogen interactions have the form



where the atom of hydrogen H is connected with two electronegative atoms X and Y. The strength of the bond, and hence its length, depend of the charge of the atoms X, H, and Y.

In the mean plane of a DNA base pair, protons are exchanged between the NH donor groups of one base and N or H acceptors of the other. So, in DNA the hydrogen bonds are of two types



and



The A-T pair contains two hydrogen bonds and the G-C pair contains three hydrogen bonds (Figure 4). Although these hydrogen bonds are weak and not highly directional [69], they contribute to the stability of the Watson-Crick-type pairing, hence have a crucial role in coding the genetic information, its transcription and replication.

Note, however, that in addition to the Watson-Crick pairing described above there is the Hoogsteen pairing: in the former, the H-bonds involve atoms or groups borne by six-membered rings of the purines only, whereas in the latter, N7 of the five-membered ring can be an acceptor.

The nature of hydrogen interactions is mainly ( $\sim 80\%$ ) electrostatic. The results of quantum-chemical calculations show that three types of forces make contributions to them: dispersion, polarization and electro-

static forces. Calculations of the total energy of hydrogen bonds give the following results for an A-T pair [70]:

$$E_{A-T} = 7.00 \text{ kcal/mol}; \quad (1.4)$$

and for a G-C pair

$$E_{G-C} = 16.79 \text{ kcal/mol}. \quad (1.5)$$

Let us compare now these energies with those of covalent bonds. Usually, the energy of hydrogen bonds is 20 or 30 times weaker than the energy of covalent bonds. As an example confirming the statement, we present here the energies of the covalent bonds C-C and C-H [71]

$$E_{C-C} = 83.1 \text{ kcal/mol}; \quad E_{C-H} = 98.8 \text{ kcal/mol}; \quad (1.6)$$

and the energy of an O-H...O bond [72]

$$E_{O-H \dots O} = 3-6 \text{ kcal/mol}, \quad (1.7)$$

so the difference between them is rather large.

There is also a marked difference in the rigidities of the bonds. To illustrate it, we can compare the energy,  $e$ , which is required to lengthen the bonds on  $0.1 \text{ \AA}$ . For covalent bonds we have [72]

$$e_{C-C} = 3.25 \text{ kcal/mol}; \quad e_{C-H} = 3.60 \text{ kcal/mol}; \quad (1.8)$$

and for an O-H...O bond we have [72]

$$e_{O-H \dots O} = 0.1 \text{ kcal/mol}. \quad (1.9)$$

So, the covalent bonds are much more rigid. On the other hand, intrabase; paired H-bonds are easily disrupted at physiological temperatures by a variety of chemical agents and physical parameters at concentrations and values commonly encountered in living systems.

#### 1.3.2 Stacking Interactions

Stacking interactions are the other type of forces which stabilize the DNA structure [73-74]. They hold one base over the next one, and form a stack of bases. According to quantum-chemical analysis, stacking interactions are contributed by dipole-dipole interactions,  $\pi$ -electron systems, London's dispersion forces and (in water solutions) hydrophobic forces. These forces result in a complex interaction pattern be-

**Table 1** Sizes of different DNA molecules

| Organism           | Number of bases    | Length, Å          | Diameter, Å |
|--------------------|--------------------|--------------------|-------------|
| <b>Viruses:</b>    |                    |                    |             |
| Polyoma or SV-40   | $5.1 \times 10^3$  | $1.7 \times 10^4$  | 20          |
| λ-phage            | $4.86 \times 10^4$ | $1.7 \times 10^5$  | 20          |
| T2-phage           | $1.66 \times 10^5$ | $5.6 \times 10^5$  | 20          |
| Viruses of cow-pox | $1.9 \times 10^5$  | $6.5 \times 10^5$  | 20          |
| <b>Bacteria:</b>   |                    |                    |             |
| Mycoplasma         | $7.6 \times 10^5$  | $2.6 \times 10^6$  | 20          |
| <i>E. coli</i>     | $4.0 \times 10^6$  | $1.36 \times 10^6$ | 20          |
| <b>Eukaryotes:</b> |                    |                    |             |
| Yeast              | $1.35 \times 10^6$ | $4.6 \times 10^7$  | 20          |
| Drosophila         | $1.65 \times 10^8$ | $5.6 \times 10^8$  | 20          |
| Human              | $2.9 \times 10^9$  | $9.9 \times 10^9$  | 20          |

around this octamer. This structure is called a nucleosome core. There is also one additional histon H<sub>1</sub> which strengthens the core, and the whole structure is called a nucleosome. So, the DNA molecule in a cell looks like a chain of nucleosomes connected with one another by fragments of DNA of length 40–100 base pairs. This structure is called chromatine. The chain of nucleosomes has a solenoidal form with 3–6 nucleosomes per turn, and this solenoid forms a more condensed and helical structure which is known as a chromosme. The human chromosomes contain the double-chain DNA with total length about 2 m.

## 1.6 APPROXIMATE MODELS OF DNA STRUCTURE

As it appears from the previous sections, the structure of the DNA molecule is rather complex, but in many cases it is enough and more convenient to use some simplified (approximate) versions of the structure. Let us consider in this section the problem of constructing approximate structural models of DNA.

### 1.6.1 General Comments

When constructing approximate models it is usually assumed that they must not include all details of the DNA structure but only the most important (or dominant) structural properties of DNA. What are these properties?

1. Reading previous sections one can notice at least two general characteristics of the DNA structure. The first is that the DNA

molecule consists of long chains of atoms. The second is that these chains have nearly regular structure, that is the DNA molecule has a 'skeleton' (sugar-phosphate chain) with an accurately repeating pattern of atoms along the chain. Due to these properties DNA is to a certain extent similar to one-dimensional periodical structure which is known in physics as quasi-one-dimensional crystals. This is why Charles Bunn gave to biomolecules of such a type the poetical name: 'crystals of chains of life' [89].

2. However, in some aspects the DNA molecule is more similar to a polymer than to a crystal, because in addition to the properties mentioned above, DNA is not a rigid system, but a flexible one. So, if we want to construct a more accurate model, we must take into account the flexible nature of DNA, that is its ability to bend, to twist, to form superstructures and so on.
3. Besides a 'skeleton' with a regular alteration of atoms or atomic groups, DNA has elements of irregular structure. So, if we want to improve the model, we must take into account the irregularity of the base sequence. We can consider this irregularity as a small disturbance of the regular pattern of the 'skeleton' and use perturbation theory for mathematical treatment.

And so on. The list of properties could be continued by inserting more and more details of the internal structure. When constructing the model we can restrict ourselves by taking into account only the first property in the list, or the first two properties, and so on. Thus, many different approximate models may be constructed describing DNA with different degrees of accuracy. The choice of the approximation depends on the conditions and the aim of the investigation. For example, if we are interested in the mobility of the DNA molecule as a whole in the solution, or the penetration of the molecule through some channel, or the mechanism of forming superhelical DNA structure, it is enough to consider the DNA molecule as an elastic filament. If, however, we are interesting in the problem of protein-DNA recognition or transcription we need to take into account some more details of the internal structure such as the helicity or the inhomogeneity due to the sequence of bases.

### 1.6.2 Hierarchy of Structural Models

To describe different structural models of the DNA molecule it is convenient to use another approach. In this approach the DNA structural

1622  
735  
1989

# Electrical Properties of Biopolymers and Membranes

**Shiro Takashima**

Department of Bioengineering  
University of Pennsylvania



Adam Hilger, Bristol and Philadelphia

All rights reserved. No part of this publication may be reproduced, stored in a retrieval system or transmitted in any form or by any means, electronic, mechanical, photocopying, recording or otherwise, without the prior permission of the publisher. Multiple copying is only permitted under the terms of the agreement between the Committee of Vice-Chancellors and Principals and the Copyright Licensing Agency.

*British Library Cataloguing in Publication Data*

Takashima, Shiro

Electrical properties of biopolymers and membranes

1. Biopolymers. Electrical properties.

I. Title

574.19'24

ISBN 0-85274-136-7

*Library of Congress Cataloging-in-Publication Data*

Takashima, Shiro, 1923-

Electrical properties of biopolymers and membranes.

Includes bibliographies and index.

1. Biopolymers-Electric properties. 2. Biopolymers-Dipole moments.

3. Membranes (Biology) I. Title.

[DNLM: 1. Electrophysiology. 2. Membranes-physiology. 3. Polymers. QT34 T136e]

QP517.B53T35 1989 574.19'127 88-34773

ISBN 0-85274-136-7

The author and IOP Publishing Ltd have attempted to trace the copyright holder of all the figures and tables reproduced in this publication and apologize to copyright holders if permission to publish in this form has not been obtained.

Published under the Adam Hilger imprint by IOP Publishing Ltd  
Techno House, Redcliffe Way, Bristol BS1 6NX, England  
242 Cherry Street, Philadelphia, PA 19106, USA

Typeset by KEYTEC, Bridport, Dorset

Printed in Great Britain by Billing and Sons Ltd, Worcester

# Contents

## Preface

### 1 The origin of dipole moment

#### 1.1 Introduction

#### 1.2 Wave functions and the dipole moment operator

#### 1.3 The calculation of $\pi$ -bond moments

#### 1.4 Polarizability

#### References and suggested reading

### 2 The polarization of groups of polar molecules

#### 2.1 Introduction

#### 2.2 The behaviour of a polar molecule in an electric field

#### 2.3 An ensemble of dipoles and polarization

#### 2.4 The concept of reaction field (Onsager theory, 1936)

#### 2.5 The dielectric constant of polar liquids (Kirkwood theory)

#### 2.6 Dipoles in solids

#### References and suggested reading

### 3 Dynamic aspects of electric polarization

#### 3.1 Introduction

#### 3.2 Electric polarization with a pulsed field

#### 3.3 The polarization of dipoles in alternating fields

#### 3.4 Intrinsic relaxation time

#### 3.5 The relaxation of solid dielectric material

#### 3.6 A generalization of relaxation theory to multiple relaxation time

#### 3.7 Use of the Gaussian distribution function

#### 3.8 Cole-Cole's empirical equation (1941)

#### 3.9 The Fuoss-Kirkwood method (1941)

#### 3.10 A treatment of dielectric relaxation using elementary rate theory (Glassstone *et al* 1941)

#### Suggested reading

#### References

JAN 8 1990

Table 5.7 Charge polarity and asymmetry in the charge distribution in proteins.†

| Protein                      | R[obs] | R[cal] > R[obs]<br>(%) |
|------------------------------|--------|------------------------|
| Ferredoxin                   | 5.04   | 5                      |
| Actinidin                    | 8.33   | 10                     |
| Concanavalin A               | 8.44   | 17                     |
| Ribonuclease A               | 5.97   | 22                     |
| Trypsin                      | 5.96   | 23                     |
| Liver alcohol dehydrogenase  | 11.34  | 26                     |
| High potential iron protein  | 4.54   | 30                     |
| Pancreatic trypsin inhibitor | 3.59   | 42                     |
| Thermolysin                  | 7.29   | 44                     |
| Carboxypeptidase             | 6.53   | 50                     |
| L-arabinose binding protein  | 7.51   | 50                     |
| Lactase dehydrogenase        | 7.43   | 66                     |
| Phospholipase A2             | 3.80   | 66                     |
| Phage T4 lysozyme            | 4.80   | 69                     |
| Subtilisin                   | 3.33   | 76                     |
| Haemoglobin $\alpha$ -chain  | 2.68   | 85                     |
| Bence-Jones protein          | 1.94   | 87                     |
| Carbonic anhydrase C         | 3.43   | 92                     |
| Flavodoxin                   | 2.41   | 94                     |
| Lysozyme                     | 1.45   | 98                     |

†Taken from Barlow and Thornton (1987). Reproduced by permission of John Wiley & Sons, Inc. © 1987.

calculated: (a) the moment due to formal charges of Asp, Glu and C-termini ( $e^-$ ); and N-termini ( $e^+$ ); (b) the moment due to partial charges of all atoms; (c) the moment due to partial charges excluding C- and N-terminal charges. Analogous to charge polarity, the expected moments due to random charge distribution are calculated and compared with the moment due to real charges. Table 5.8 shows the calculated real moments of various proteins and the percentage of  $\mu[\text{cal}]$  exceeding  $\mu[\text{obs}]$ . As before, ferredoxin ranks the first in the asymmetry list, namely, the dipole moment of this protein is disproportionately large for its size. The rank order of dipole moment is not identical to the similar list for charge polarity.

The values of dipole moments for proteins range from 100 to 700 D. However, these large values are due to the size of the proteins and are not due to the unique arrangements of charged sites in these molecules.

Table 5.8 The calculated dipole moment of various proteins.†

| Protein                               | Dipole moment<br>(D) | $\mu[\text{cal}] > \mu[\text{obs}]$<br>(%) |
|---------------------------------------|----------------------|--|
| Ferredoxin (FDX)                      | 238                  | 12   |
| Actinidin (ACT)                       | 675                  | 23   |
| Ribonuclease A (RNS)                  | 481                  | 24   |
| Pancreatic trypsin (PTI)<br>inhibitor | 269                  | 29   |
| Flavodoxin (FXN)                      | 523                  | 35   |
| Subtilisin (SBI)                      | 508                  | 45   |
| Thermolysin (TLN)                     | 711                  | 47   |
| Liver alcohol (ADN)<br>dehydrogenase  | 823                  | 58   |
| Trypsin (PTN)                         | 356                  | 61   |
| Phage T4 lysozyme (LZM)               | 407                  | 68   |
| Carbonic anhydrase C (CAC)            | 525                  | 71   |
| Carboxypeptidase (CPA)                | 492                  | 73   |
| Bence-Jones protein (BEI)             | 177                  | 74   |
| Haemoglobin $\alpha$ -chain (MNB)     | 235                  | 80   |
| High potential iron (HPI)<br>protein  | 144                  | 83   |
| Lactase dehydrogenase (LDH)           | 420                  | 91   |
| Concanavalin A (CNA)                  | 187                  | 97   |
| Lysozyme (LYZ)                        | 111                  | 97   |
| L-arabinose binding (ABP)<br>protein  | 239                  | 98   |
| Phospholipase A2 (BPA2)               | 103                  | 98   |

†Taken from Barlow and Thornton (1987). Reproduced by permission of John Wiley & Sons, Inc. © 1987.

It is a simple task to demonstrate that these moments can be generated by placing one or two charge pairs diametrically across protein molecules. Figure 5.30 shows the calculated dipole moments of proteins plotted against molecular diameters. In addition, the dipole moments which are generated by hypothetical charge pairs located diametrically are shown. Line A is due to one charge pair, line B due to two charge pairs and line C is due to three charge pairs. As shown, all of the dipole moments for protein fit within the area bounded by lines A-C. There are a few exceptions such as lysozyme whose dipole moments are even below the hypothetical moment due to one charge pair. This means that the centres of positive and negative charges in this protein are almost identical.

In spite of Barlow and Thornton's detailed calculation of the dipole

differences alone. The relaxation was attributed by these workers to the dipole moment in the transverse axis of the DNA fibre. This conclusion seemed quite reasonable at that time, based on the magnitude of the dipole moment and the value of relaxation time. The interpretation of the dielectric behaviour of a DNA molecule, however, was drastically modified later as new experimental results began to appear in the literature.

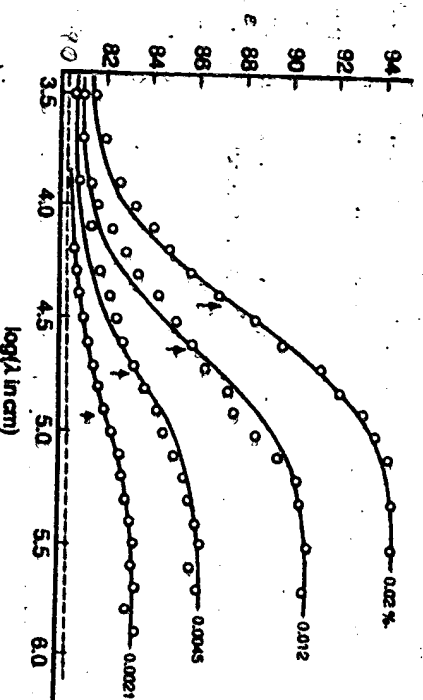


Figure 7.3 Dielectric dispersion data for a small DNA molecule. The abscissa is the wavelength, instead of frequency. (From Allgen 1950.) Reproduced by permission of *Acta Physiologica Scandinavica*.

The dielectric behaviour of nucleohistone (DNH) was studied by the same authors. Histone is a basic protein with which DNA forms a tight complex *in vivo*. The complexation of DNA with histone is expected to alter the charge distribution and, consequently, the value of the dipole moment. The dielectric dispersion curves of nucleohistone are shown in figure 7.4. The dielectric increment of DNH is, as expected, smaller than that of DNA. This result proves that the presence of histone molecules shields the charges of DNA and decreases its dipole moment. The dielectric measurements performed by Allgen and co-workers are the only source of information as to the dielectric behaviour of DNH. These data were, however, obtained many years ago. Since then the technique of purification of nucleic acids has been improved greatly. While the dielectric properties of purified DNA have been investigated repeatedly by many other researchers and new information on the nature of the dipole moment has been available, the dielectric properties of nucleohistone have never been reinvestigated.

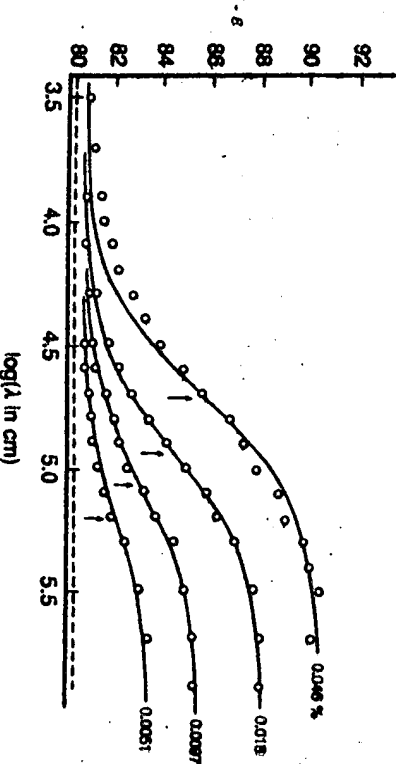


Figure 7.4 Dielectric dispersion data for nucleohistone (DNH). (From Allgen 1950.) Reproduced by permission of *Acta Physiologica Scandinavica*.

The research by Jungner and co-workers was performed, as already mentioned, even before the double helical structure of DNA became known. These early dielectric measurements of DNA were handicapped for two reasons.

(i) The technique of DNA purification was not adequate at that time. In fact, early investigators used very small DNA samples which might have been fragmented during purification. Recent measurements are all performed using much larger and/or more uniform DNA samples. The conclusion that DNA has a dipole moment in the direction of the transverse axis may have been due, at least partly, to their use of small DNA preparations.

(ii) The structure of the DNA molecule was not well documented at that time. Therefore, the interpretation of experimental results was made difficult because of the lack of sufficient knowledge about the structure.

In spite of these shortcomings, however, the research done by these early workers is highly significant as a landmark for this field.

Subsequently, interesting measurements of the dielectric constant of DNA solution were performed using rotating electrodes by Jacobson (1953) and Jerrard and Simmons (1959). These investigators measured the change in the dielectric constant of DNA solution due to the alignment caused by velocity gradients. For example, Jacobson observed an increase in the dielectric constant of DNA solution when an electrical field is applied along the laminar flow. On the other hand, a decrease in dielectric constant was noted when electrical fields were applied across the flow. The results obtained by Jerrard and Simmons are similar to

those obtained by Jacobson. These results are a clear indication that DNA has a dipole moment in the direction of the longitudinal axis. This conclusion is in contrast to the one reached by Jungner and co-workers some years earlier. As will be discussed shortly, the conclusion that DNA has a longitudinal dipole moment has been confirmed by more recent investigations. Both Jungner and co-workers and Jacobson postulated that DNA had a permanent dipole moment, a concept which was contested later by other investigators. Detailed discussions on rotating electrodes are also found in the following references: Peterlin and Reinhold (1965), Saito and Kato (1957), Takashima (1970) and Barissas (1974).

#### 7.4 Dielectric Properties of DNA at Low Frequencies

Starting in the early 1960s, Takashima (1963, 1966, 1967) performed a series of measurements on the dielectric constant of highly polymerized DNA samples (with a molecular weight of about  $2-3 \times 10^6$ ) in a wide frequency range, which had never been attempted earlier. The range he covered was between 20 Hz and 200 kHz. The lowest frequency used by Jungner and co-workers was 100 kHz. Therefore, the overlap of frequency ranges used by these investigators is only slight. Takashima observed that the dielectric constant of DNA solution increased markedly below 1 kHz and reached a value of 1500 or more at a concentration of only 0.01%. One of the results obtained by Takashima is illustrated in figure 7.5. Note the rise of the dispersion curve below 1 kHz. Also note that the dispersion curve is still rising even at 20–30 Hz. The low-frequency plateau was obtained using the Cole-Cole plot, as shown by the inset of this figure. The dipole moment can be roughly estimated using (5.23) and a value of as large as 100 000 D was found. Based on this observation, it was concluded that the primary dispersion of DNA is located in the 50–100 Hz region and that the small dispersion observed by Jungner and co-workers may have been a secondary dispersion of unknown origin.

It has been mentioned previously that DNA undergoes a transition from the helical configuration to a random-coil structure upon heating at 80–95 °C. Heating, acidic pH and low ionic strength cause unwinding of the double strands and trigger a phase transition. Double helical DNA has a highly ordered internal structure with a remarkable regularity. In other words, helical DNA is in a crystalline state. On the other hand, single strand DNA is a random-coil polymer with no internal regularity, that is to say, single strand DNA is an amorphous substance. Therefore, the helix-coil transition is analogous to the melting of crystals.

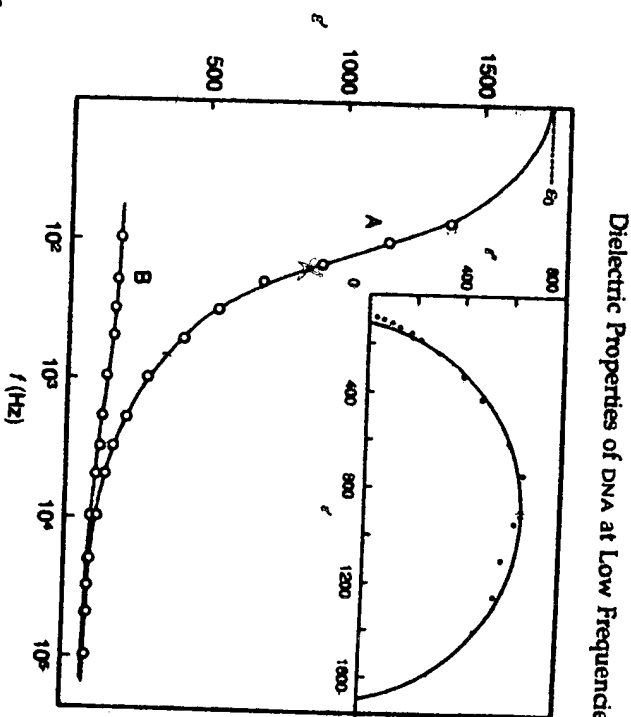


Figure 7.5 The dielectric dispersion of a highly polymerized DNA molecule. Curves: A, double helical DNA; B, single strand random-coil DNA. The inset shows the Cole-Cole plot of the same sample. Reproduced with permission from Takashima (1966). Copyright (1966) American Chemical Society.

The dielectric properties of random-coil DNA have also been investigated by Takashima (1966) and one of his results is shown in figure 7.5, along with that of helical DNA. Even a cursory examination is sufficient to recognize the difference between these two curves. The extraordinarily large dielectric increment of helical DNA is replaced by a small increment upon the helix-coil transition, i.e. from an increment of 1500 to about 20 dielectric units at a concentration of 0.01%. The main feature of the helix-coil transition is the melting of the helix backbone. Therefore, the drastic decrease of dielectric increment following the phase transition is clearly due to the collapse of the secondary structure of helical DNA. In other words, the exceedingly large dielectric increment indicates that the dipole moment of helical DNA is in the direction of the major axis. Application of an electrical field to DNA solution will cause either the orientation of the entire molecule or the fluctuation of mobile ions along the major helical axis. This explanation is consistent with the large relaxation time observed by Takashima.

Let us recall the Watson-Crick model shown in figure 7.1. According to this model, DNA consists of two nucleotide strands. However, geometric constriction requires these two strands to be anti-parallel.

Only an anti-parallel configuration makes these strands compatible to each other without steric hindrance. Nucleotides are basically a polar polymer chain. Although there is no experimental evidence, it is quite reasonable to assume that a single nucleotide chain has a large permanent dipole moment because of the repeating polar structural units, with the polarity in one direction. The DNA samples which were used for the measurements have a molecular weight of about  $3 \times 10^6$ . This can be translated into an extended length of approximately  $2 \mu\text{m}$ . Since the distance between base planes is  $3.4 \text{ \AA}$ , there are about 5900 such repeating units in one DNA molecule. If the total dipole moment of DNA is divided by this number, we find the net dipole moment per each  $3.4 \text{ \AA}$  unit to be 20 D. Since base pairs are stacked with their molecular plane perpendicular to the helical axis, the dipole moment of base molecules in the direction of the helical axis (the  $z$ -direction) is nearly zero except for a slight distortion of the base planes. Therefore, the dipole moment of 20 D must arise from phosphate groups. As mentioned before, nucleotide chains in helical DNA are anti-parallel to one another, in other words, the polarity or dipole moment of one chain opposes the moment of the other chain. Under these circumstances, it is difficult to attribute the large dipole moment to particular groups or structures in the DNA molecule. The origin of the dipole moment of DNA must be sought from different sources such as an induced dipole moment by ion fluctuation. The dipole moment due to ion fluctuation was discussed in Chapter 6. In small globular proteins, the magnitude of the ion fluctuation moment is negligibly small compared with the permanent dipole moment. However, the same argument will not hold for large fibrous polymers such as DNA where the effective distance of ion fluctuation is very long.

In the above, we found that helical DNA has an exceedingly large dipole moment and that the dipole moment disappears upon a helix-coil transition, an indication that the secondary structure has an important bearing on the large dipole moment. Other evidence which supports this statement was found from the length dependence of the dipole moment of DNA. DNA fibres were fragmented using sonic vibration and the mean lengths of DNA samples were estimated from the rotary diffusion constant. The rotary diffusion constant of an elongated polymer is related to its length by the following equation (Perrin 1934):

$$\Theta = \frac{3kT}{16\pi\eta a^3} [2\ln(2a/b) - 1] \quad (7.1)$$

where  $a$  and  $b$  are the major and minor axes of the rod and  $\eta$  is the viscosity. Assuming that the transverse axis of double helical DNA is constant at about  $20 \text{ \AA}$ , we can solve this equation numerically. For short DNA, the rigid rod approximation is justified and (7.1) can be used without serious error. Figure 7.6 shows the results of these experiments.

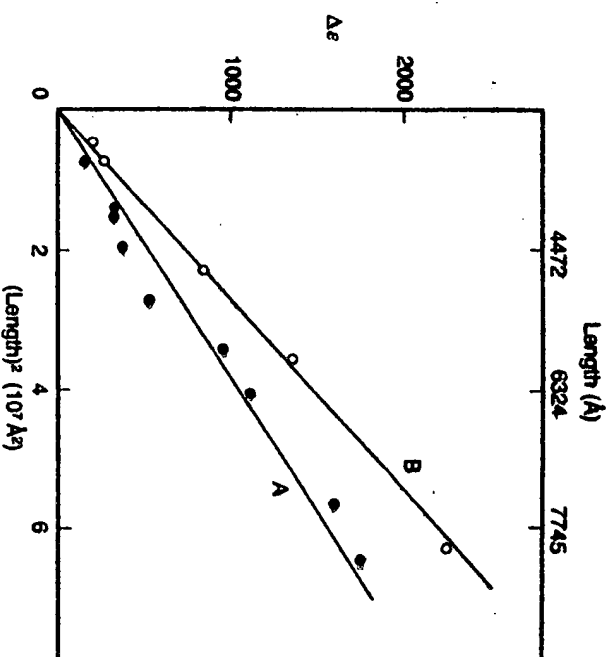


Figure 7.6 A plot of the dielectric increment against hydrodynamic length for salmon sperm (curve A) and calf thymus (curve B) DNA. Note the linear relationship between  $\Delta\epsilon$  and  $L^2$ . Reproduced with permission from Takashima (1966). Copyright (1966) American Chemical Society.

Clearly, the dielectric increment is proportional to the square of the effective length of DNA, an indication that helical DNA has a large longitudinal dipole moment. In addition, as shown in figure 7.7, the relaxation time is proportional to the square of the effective length. As we recall, the polarization of polar molecules is in general due to the orientation of the entire molecule if a permanent dipole is a dominant component. Thus, the relaxation time, under this condition, would be proportional to the cube of the effective length of the molecule (see figures 5.9 or 5.18). The relaxation time of DNA was, unexpectedly, found to be proportional to the square of length. This observation raises a serious question as to the nature or the origin of the dipole moment of DNA molecules. It was shown in Chapter 6 that the relaxation time due to ion fluctuation has a quadratic size dependence. In view of the theoretical considerations and the experimental observations, there is a strong indication that the dielectric relaxation of DNA is due to some process other than the orientation of a permanent dipole. DNA is a highly charged rod-like polymer surrounded by counterion clouds. Thus, counterion polarization may be the possible mechanism for the relaxation of DNA. Let us look at (6.137) which was derived by Schwarz (1962)



# Structure of Plectonemically Supercoiled DNA

T. Christian Bolest†

Department of Molecular Biology  
University of California, Berkeley  
Berkeley, CA 94720 U.S.A.

James H. White

Department of Mathematics  
University of California  
Los Angeles, CA 90024 U.S.A.

and Nicholas R. Cozzarelli

Department of Molecular and Cell Biology  
Division of Biochemistry and Molecular Biology  
University of California  
Berkeley, CA 94720 U.S.A.

(Received 29 August 1989; accepted 11 December 1989)

Using electron microscopy and topological methods, we have deduced an average structure for negatively supercoiled circular DNA in solution. Our data suggest that DNA has a branched plectonemic (interwound) form over the range of supercoiling tested. The length of the superhelix axis is constant at 41% of the DNA length, whereas the superhelix radius decreases essentially hyperbolically as supercoiling increases. The number of supercoils is 89% of the linking deficit. Both writhe and twist change with supercoiling, but the ratio of the change in writhe to the change in twist is fixed at 2.6 : 1. The extent of branching of the superhelix axis is proportional to the length of the plasmid, but is insensitive to superhelix density. The relationship between DNA flexibility constants for twisting and bending calculated using our structural data is similar to that deduced from previous studies. The extended thin form of plectonemically supercoiled DNA offers little compaction for cellular packaging, but promotes interaction between *cis*-acting sequence elements that may be distant in primary structure. We discuss additional biological implications of our structural data.

## 1. Introduction

DNA supercoiling, the coiling of the axis of the double helix, is ubiquitous in biological systems. It arises in two ways. It can result from winding around proteins, as in eukaryotic nucleosomes. Supercoiling can also result from the topological constraint imposed upon underwound or overwound closed molecules free in solution. Both sources of supercoiling are important *in vivo*.

The topological properties of closed circular DNA provide a conceptual framework for understanding supercoiling (for a review, see Cozzarelli *et al.*, 1990).

The number of times the two strands of the DNA double helix are intertwined, i.e. the linking number of the DNA ( $Lk$ ), is a constant that can be changed only by breaking the DNA backbone. Although  $Lk$  is a topological property, it is the sum of two geometric parameters that describe the shape of the DNA, writhe ( $Wr$ ) and twist ( $Tw$ ) (White, 1969):

$$Lk = Wr + Tw. \quad (1)$$

$Wr$  is a measure of the coiling of the DNA axis, and  $Tw$  reflects the helical winding of the DNA strands around each other. For circular DNAs isolated from natural sources, supercoiling is a geometric compensation for a deficiency in linking number. There is an unfavorable free energy associated with decreasing  $Lk$  from the preferred value of the

† Present address: Graduate Department of Biochemistry, Brandeis University, Waltham MA 02254, U.S.A.

## 2. Experimental Procedures

### (a) DNA

For electron microscopy, 2 plasmids, differing in size by a factor of 2, were studied. Both are derivatives of pBR322 (Bolivar *et al.*, 1977; Sutcliffe, 1979). pAB7.0d is 6978 bp† in length (Wasserman *et al.*, 1988), and pJB3.5d is 3480 bp in length (Bliska & Cozzarelli, 1987).

For experiments using site-specific recombination catalyzed by the lambda integrase system (Int), 2 additional plasmids were used, pJB3.5i (3459 bp; Bliska, 1988) and pBNW3.8d (3800 (±50) bp; Wasserman *et al.*, 1988). All 4 plasmids contain the *attP* and *attB* recombination sites of the Int system. In pJB3.5d and pBNW3.8d, the recombination sites are oriented as direct repeats. With these substrates, Int recombination produces dimeric catenanes. pJB3.5i is a derivative of pJB3.5d in which the recombination sites are oriented as inverted repeats; recombination of this substrate gives knotted products. For pJB3.5d, pJB3.5i and pBNW3.8d, the distances between the recombination sites are 574, 515 and 900 (±50) bp, respectively (Bliska, 1988; Bliska & Cozzarelli, 1987; Wasserman *et al.*, 1988).

Large-scale plasmid purification was performed using the alkaline lysis method, followed by 2 cycles of ethidium bromide/CsCl equilibrium density-gradient centrifugation (Maniatis *et al.*, 1982).

### (b) Topoisomerase reactions and measurement of $\Delta Lk$

To prepare plasmid samples with defined levels of supercoiling, DNA (100 µg/ml) was relaxed in the presence of 0 to 8 µg ethidium bromide/ml and with a 5-fold excess of wheat germ topoisomerase I (Dyan *et al.*, 1981) over that necessary for full relaxation. In early experiments using electron microscopy, relaxation was carried out in Topo I buffer (50 mM-Tris·HCl (pH 8.0), 50 mM-NaCl, 1 mM-dithiothreitol, 1 mM-EDTA) for 30 min at 37°C. For later electron microscopy experiments, reactions were performed in TE buffer (10 mM-Tris·HCl (pH 8.0), 1 mM-EDTA) for 30 min at 25°C. For experiments using Int site-specific recombination, relaxations were performed at 25°C in Int buffer (20 mM-Tris·HCl (pH 8.0), 50 mM-NaCl, 10 mM-MgCl<sub>2</sub>). Reactions were terminated by addition of sodium dodecyl sulfate to 1% (w/v) final concentration. Protein and ethidium bromide were removed by 3 extractions with phenol, and the DNA was precipitated with ethanol.

Linking number difference was measured by the band counting method (Keller, 1975; Shure & Vinograd, 1976). A series of 0.8% (w/v) agarose gels (40 mM-Tris-acetate (pH 7.8), 5 mM-sodium acetate, 2 mM-EDTA) containing from 0 to 40 µg chloroquine phosphate/ml were run at 1.3 V/cm for 24 h with buffer recirculation to resolve sample topoisomer distributions. Gels were stained with ethidium bromide and photographed under short-wave ultraviolet light. Photographic negatives were scanned with a Zeineh soft laser densitometer.

The linking difference,  $\Delta Lk$ , is the difference between the average  $Lk$  of a sample and the average  $Lk$  after relaxation,  $Lk_0$ . Relaxation is obtained by topoisomerase treatment under temperature and buffer conditions identical to those used to analyze the sample. To facilitate comparisons between plasmids of different size, linking

deficits will usually be expressed using the size independent descriptor,  $\sigma$ , where:

$$\sigma = \frac{(Lk - Lk_0)}{Lk_0} = \frac{\Delta Lk}{Lk_0} \quad (2)$$

For most of the electron microscopy, DNA samples that were relaxed in Topo I buffer at 37°C were spread for electron microscopy in TE buffer at 25°C. In some experiments, the same samples were spread in Int reaction buffer at 25°C. To correct for changes in  $\sigma$  caused by differences in temperature and solution conditions, we compared the  $Lk$  values for samples relaxed under these 3 conditions. The change in  $\sigma$  was -0.003 for transfer from Topo I buffer at 37°C to TE at 25°C. For transfer from Topo I buffer at 37°C to Int buffer at 25°C, the change in  $\sigma$  was -0.007. All reported  $\sigma$  values have been corrected using these conversion factors and refer to the superhelical density under the buffer and temperature conditions used for spreading.

### (c) Electron microscopy

Electron microscopy was performed using the polylysine adsorption method of Williams (1977). Samples were prepared at room temperature (25°C). Briefly, carbon-coated formvar grids were exposed to high-voltage glow discharge at 70 to 100 mTorr (1 Torr ≈ 133.322 Pa) for 20 s and then coated with poly-L-lysine (Sigma Chemical Co.) by adding 8 µl of a 1 µg/ml solution for 1 min. The grids were drained and air-dried by aspiration with a drawn-out Pasteur pipette. An 8-µl drop of DNA solution (0.5 to 5 µg DNA/ml) was added to the grid and allowed to adsorb for 1 min. This was followed by a 20 s wash in 0.1 M-ammonium acetate, staining in 5% (w/v) uranyl acetate for 20 s, and a 5 s wash in 0.01 M-ammonium acetate. The grids were rapidly air-dried by aspiration and rotary shadowed with tungsten. Micrographs were taken at a primary magnification of 33,000× using a JEOL100CX electron microscope.

### (d) Measurement of electron micrographs

Most of the measurements were performed on photographic prints (final magnification 82,500×) using an electronic digitizer (Numonics). To measure the number of DNA crossings/DNA molecule, also called nodes, negatives were projected onto paper (final magnification 330,000×), the path of the DNA was traced, and the nodes were counted from the tracings.

The variation introduced by using different grids for each DNA sample was estimated by comparing the average lengths of nicked molecules on each grid. The grid-to-grid variation in these measurements was, at most, 5% of the average total length. To minimize the effect of this variation, we normalized all data from a grid using the average length of nicked molecules on the same grid. We assume this length to be the number of base-pairs in the plasmid multiplied by 3.35 Å per base-pair, or 23,380 Å for pAB7.0d and 11,660 Å for pJB3.5d (1 Å = 0.1 nm). These values are within 5% of the lengths measured using the nominal magnification of the microscope.

The superhelix axis is defined as the line that passes through the nodes and bisects the area enclosed by the DNA between adjacent nodes. Because of the regular shape of the supercoils, the path of this line could be determined unambiguously and, therefore, it was drawn freehand. Fig. 2 shows a typical electron micrograph of a

† Abbreviations used: bp, base-pair(s); IHF, integrative host factor; kb, 10<sup>3</sup> bases or base-pairs.

(Craigie & Mizuuchi, 1986; Drüge & Cozzarelli, 1989; Kanaar *et al.*, 1989). The most convincing evidence for this proposal is that productive site alignment in these systems, which normally require negative supercoiling, can also be achieved in catenanes or knots where the sites have a similar interwound geometry.

The interwound form may have significance for transcriptional regulation as well. A number of genes have regulatory elements that involve two or more *cis*-acting DNA sites, which may be separated by thousands of bases of DNA. One commonly cited mechanism for interaction between these sites is the formation of a DNA loop between the sites (Besse *et al.*, 1986; Dunn *et al.*, 1984; Hochschild & Ptashne, 1986; Irani *et al.*, 1983; Reitzer & Magasanik, 1986). If this loop can be the end of a plectonemic branch, then the interaction between the sites could be regulated by the level of supercoiling in a way that is analogous to that proposed above for site-specific recombination systems. For the *lac* repressor and the AraC protein, there is direct evidence that supercoiling can promote looping (Hahn *et al.*, 1986; Whitson *et al.*, 1987).

Another important feature of the interwound form is the branch point. At the branch point, three distant DNA segments are brought into close proximity. This feature is important for regulatory systems where three different *cis*-acting DNA elements are involved, such as the G-inversion system of bacteriophage Mu (Kanaar *et al.*, 1988, 1989) and Mu transposition (Leung *et al.*, 1989). It could also be important for regulation of transcription of genes that have multiple separate promoter/enhancer elements.

While the most dramatic and obvious effect of negative supercoiling is the change in the overall

geometry of the DNA, there are clear, concomitant changes in the structure of the double helix. This is seen in the smooth change of  $Tw$  (eqn (13)) and helical repeat (White *et al.*, 1988) with  $\sigma$ . These changes could affect DNA-protein interactions in at least two ways. First, changing  $Tw$  and helical repeat will tend to cause concomitant changes in other aspects of double-helical structure such as the inclination angle of the bases and their exposure in the grooves. These changes, in turn, would influence recognition by sequence-specific DNA binding proteins. Second, the change in double-helical structure will alter the phasing between adjacent *cis*-acting sequences. These are critically important for correct protein-protein interactions in specialized nucleoprotein complexes (Bellomy *et al.*, 1988; Echols, 1986; Hochschild & Ptashne, 1986; Johnson *et al.*, 1987).

In conclusion, whereas the interwound form of supercoiling is a particularly poor storage form, it is an excellent form for the active state of DNA. Thus, the two forms of supercoiling may denote regions of specialized function within the chromosome. It is interesting to compare the genome activity and packaging in prokaryotes and eukaryotes. In prokaryotes, a large fraction of the genome is undergoing transcription or replication, whereas in the differentiated cells of eukaryotes, replication has ceased, and only 5 to 10% of the genome is being transcribed (for a review, see Davidson, 1977). This dramatic difference in genome activity is reflected in DNA packaging; in prokaryotes, it has been estimated that 40% of the DNA is plectonemically supercoiled (Bliska & Cozzarelli, 1987), but in eukaryotes, the vast majority of the DNA is solenoidally wound in nucleosomes.

## APPENDIX

### Quantification of the Site-specific Recombination Assay for Supercoil Number

During intramolecular recombination by the lambda Int system, a portion of the substrate supercoils are converted to product catenanes or knot interlinks (Fig. 4). Here, we derive an equation that relates the number of product catenane interlinks to the total number of supercoils in the substrate. The equation for knotting is exactly analogous. We revise and expand the earlier treatment by Benjamin & Cozzarelli (1986) to address branched molecules and to give more accurate values for molecules with few supercoils.

The *att* sites divide the recombination substrates into two domains, indicated as open and shaded regions in Figure 4. Considering the lateral view shown in Figure 4, nodes formed between DNA segments from different domains are called inter-

domainal. The number of catenane nodes in the products,  $Cn$ , is determined by the number of interdomainal nodes in the substrate at recombination. These nodes are formed in two ways. A small, fixed number are introduced by the wrapping of the DNA about the enzyme and by the strand exchange mechanism and are denoted  $^{icr}X_{enz}$ . The second component is due to interdomainal substrate supercoiling outside the enzyme-DNA complex that is trapped at site synapsis,  $^{icr}X_s$ . The sum of these two components determines  $Cn$  (Cozzarelli *et al.*, 1984):

$$Cn = ^{icr}X_{enz} + ^{icr}X_s.$$

We are interested in how  $Cn$  varies with  $\Delta Lk$  and assume that  $^{icr}X_{enz}$  is constant. Thus, the change in  $Cn$  reflects only the change in  $^{icr}X_s$ .

**DNA TOPOLOGY AND ITS BIOLOGICAL EFFECTS**

Monograph 20

Copyright 1990 by Cold Spring Harbor Laboratory Press

All rights reserved

Printed in the United States of America

Book design by Emily Harste

**Library of Congress Cataloging-in-Publication Data**

DNA topology and its biological effects / edited by

Nicholas R. Cozzarelli, James C. Wang.

p. cm. — (Cold Spring Harbor monograph series; 20)

Includes bibliographical references.

ISBN 0-87969-348-7

1. DNA—Conformation 2. DNA topoisomerase II. 3. DNA topoisomerase II.

I. Cozzarelli, Nicholas R. III. Wang, James C. III. Series.

[DNLM: 1. DNA Untwisting Proteins—physiology. QU 58 D6298]

QP624.D175 1990

574.873282—dc20

DLC

for Library of Congress

90-1540

CIP

**D. HIDDEN RAMSEY LIBRARY  
U.N.C. AT ASHEVILLE  
ASHEVILLE, N. C. 28814**

Authorization to photocopy items for internal or personal use, or the internal or personal use of specific clients, is granted by Cold Spring Harbor Laboratory Press for libraries and other users registered with the Copyright Clearance Center (CCC) Transactional Reporting Service, provided that the base fee of \$1.00 per article is paid directly to CCC, 27 Congress St., Salem MA 01970. [0-87969-348-7/90 \$1.00 + .00]. This consent does not extend to other kinds of copying, such as copying for general distribution, for advertising or promotional purposes, for creating new collective works, or for resale.

All Cold Spring Harbor Laboratory Press publications may be ordered directly from Cold Spring Harbor Laboratory, Box 100, Cold Spring Harbor, New York 11724. (Phone: 1-800-843-4388.) In New York State (516) 367-8325. FAX: (516) 367-8432.

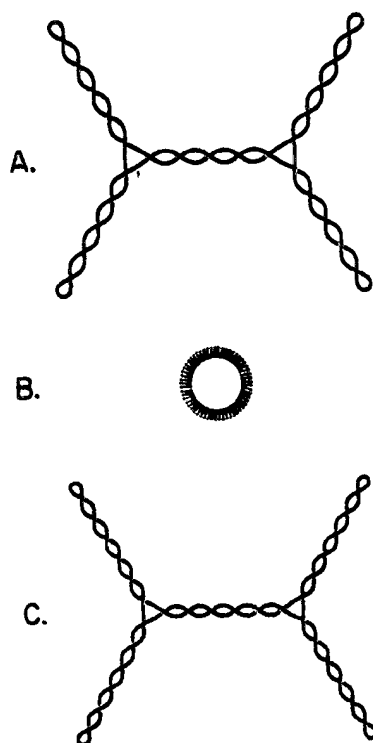


**Figure 15** Scale drawings for plectonemic and solenoidal supercoiled DNA models. Parts A and C are scale drawings of plectonemic DNA in solution, and part B is a model for nucleosomal DNA. The value of  $\sigma$  is  $-0.06$  in part A and  $-0.079$  in parts B and C. In all cases, the length of the DNA is  $15,500 \text{ \AA}$  ( $4.6 \text{ kb}$ ), and the diameter of the DNA is taken to be  $22 \text{ \AA}$ . All dimensions are to scale except that the diameter of the DNA duplex in part B has been reduced by 50% for the sake of clarity. For the plectonemic DNA, the length of the plectonemic axis is  $6300 \text{ \AA}$ , and the superhelix radius is  $56 \text{ \AA}$  in part A and  $43 \text{ \AA}$  in part C. For both, there are two branch points that result in a total of four ends. To model nucleosomal DNA, we imagine the DNA to be solenoidally supercoiled with nucleosomal geometry. This model is equivalent to a hypothetical case in which nucleosomes form a continuous end-to-end stack with no linker DNA. We have assumed 81-bp/superhelical turn, giving a total of 57 supercoils in 4.6 kb. The superhelix radius is  $43 \text{ \AA}$ , the radius of the torus axis is  $250 \text{ \AA}$ , and the length of the torus axis is  $1600 \text{ \AA}$ . Notice the striking difference in compaction for the two forms of DNA supercoiling.

is energetically at a minimum when  $\gamma = 54^\circ$ . The geometric relationship between  $L$ , the length of the DNA, and the superhelix parameters for our model is given by the formula

## Harmonic and subharmonic resonances of microwave absorption in DNA

Chun-Ting Zhang

*Center of Theoretical Physics, Chinese Center of Advanced Science and Technology (World Laboratory)  
and Department of Physics, Tianjin University, Tianjin, China*

(Received 4 November 1988; revised manuscript received 10 April 1989)

We have studied theoretically the movement of large molecular groups of DNA double helices in solution, which are driven by the electromagnetic field. The longitudinal vibration of nucleotides and the torsional movement of bases are taken into account at the same time. A set of coupled nonlinear partial differential equations has been established, and we have solved these equations by the method of perturbation. The result shows that there exists resonant absorption of microwave energy for both longitudinal and torsional modes. The resonant frequencies for the former and the latter are in the region of gigahertz and subterahertz, respectively. In addition to an  $n$ th-harmonic resonance at  $\omega_n$ , our theory also predicts a subharmonic resonance at  $\omega_n/2$ . The strength of the latter is proportional to  $l^{-3}$ , where  $l$  is the length of DNA. The necessary conditions to observe these resonances are also discussed.

### I. INTRODUCTION

Edwards, Davis, Saffer, and Swicord<sup>1</sup> (EDSS) have reported in 1984 a very important experimental result on the demonstration of resonant absorption of microwave energy by aqueous solutions containing DNA in the region of several gigahertz. The resonances observed by EDSS have been assigned to the longitudinal acoustic waves driven by a microwave field in DNA.<sup>2</sup> Although their result is still controversial,<sup>3</sup> the work of EDSS has attracted a lot of attention theoretically. The theory of DNA lattice dynamics proposed by Prohofsky and co-workers since 1974 seems to be the most accurate and detailed theory for DNA (Ref. 4) (see also Ref. 2 and the references therein). The theory takes into account the helical conformation and all atoms besides the hydrogen in the unit cell. One of the key problems related to the EDSS experiment is the damping caused by the viscosity of water. Van Zandt and co-workers have developed a series of theories of the hydration layer around the polymer to explain the result of EDSS.<sup>5,6</sup> A theory of nonlinear dynamics proposed by Scott and co-workers has been used successfully to explain several outstanding experimental facts.<sup>7-10</sup> However, only one degree of freedom—the longitudinal displacement—was taken into account in Scott's theory. It is the purpose of this paper to consider another degree of freedom in addition to the longitudinal one. It is well known that the longitudinal vibration of nucleotides, the rotation of bases (base rotator) around the axis parallel to the helical axis, and the sugar pucker are the main degrees of freedom for B-DNA.<sup>11</sup> In fact, Krumhansl and Alexander have developed dynamical equations in considerable detail for these degrees of freedom.<sup>11</sup> We think that the sugar pucker is important for the A-B-DNA transition; however, it is less important for the microwave absorption. Therefore we shall neglect the sugar pucker in our calculation.

The rotation of bases has been studied by England *et al.*,<sup>12</sup> Yomosa,<sup>13</sup> Homma and Takeno,<sup>14</sup> and Zhang in addition to the work of Krumhansl and Alexander mentioned above. It is well known that the permanent dipole moments of bases are considerably large. According to Devoe and Tinoco,<sup>16</sup> the permanent dipole moments for bases A, G, T, and C are (in units of  $D$ ) 2.8, 6.3, 3.5, and 8.0, respectively. The coupling of the external electric field with these dipole moments may produce a moment of force for each base. So a torsional acoustic wave propagating along the DNA chain may occur. In this paper we would like to point out the possibility that a torsional acoustic wave driven by a microwave field in aqueous solution containing DNA may exhibit a series of resonances in the region of subterahertz frequencies. We shall deal with the resonances of longitudinal waves observed by EDSS and the resonances of torsional wave predicted theoretically in a unified form. This paper is organized as follows. In Sec. II we introduce the Hamiltonian and the coupled dynamic equations to be studied. In Sec. III the equations are solved by a method of perturbation. In Sec. IV the parameters in this theory are estimated. In Sec. V some discussions and conclusions are discussed.

### II. HAMILTONIAN AND EQUATIONS OF MOTION

Let  $\varphi_n$  and  $\varphi'_n$  be the rotation angle of the  $n$ th base rotator and of its complementary one, respectively, as Refs. 11-15. For simplicity the case of  $|\varphi_n| = |\varphi'_n|$  will be taken into account only hereafter. In this case, the Hamiltonian  $H_\varphi$  related solely to  $\varphi_n$  takes the form

$$H_\varphi = 2 \sum_n \left[ \frac{1}{2} I \dot{\varphi}_n^2 + V(\varphi_n) + \frac{1}{2} S (\varphi_n - \varphi_{n-1})^2 \right], \quad (2)$$

where  $I$  is the mean value of the moments of inertia of the base rotator,  $S$  is the stacking energy of bases, and  $V(\varphi_n)$

# Thermal and Nonthermal Mechanisms of Interaction of Radio-Frequency Energy with Biological Systems

Kenneth R. Foster, *Fellow, IEEE*

*Invited Paper*

**Abstract**—This paper reviews thermal and nonthermal mechanisms of interaction between radiofrequency (RF) fields and biological systems, focusing on pulsed fields with high peak power but low duty cycle. Models with simplified geometry are used to illustrate the coupling between external electromagnetic fields and the body, and with cellular and subcellular structures. Mechanisms of interaction may be linear or nonlinear with field strength, and thermal or nonthermal. Each mechanism is characterized by a threshold field strength (below which no observable response is produced) and time constant of response. Several classes of nonthermal mechanisms of interaction are well established; however, the anticipated thresholds for producing observable effects are expected to be very high. The bioeffects literature contains many open questions, including many reports of effects that are not clearly interpretable in terms of the mechanisms discussed in this paper.

## I. INTRODUCTION

SEVERAL thousand studies have examined the interactions between radio-frequency (RF) electromagnetic fields and biological systems, motivated both by beneficial applications and also possible hazards of such energy [1]. Most of these studies have employed continuous wave or pulsed sources with modest peak field strengths. Under such conditions, the dominant effects arise from thermal mechanisms.

The focus of this Special Issue is on nonthermal effects, i.e., effects produced directly by the applied fields rather than indirectly as a result of heating, particularly those that might be elicited by pulsed fields of very high peak strength. Several papers in this Special Issue concern possible biomedical applications of ultrawide-band (UWB) pulse generators, which can produce electric fields in air of tens of kV/m with risetimes of the order of 1 ns [2]. EMP simulators, which date back to the 1970's, can generate fields as high as 60–100 kV/m with pulse durations of 100–300 ns. The issue of nonthermal effects is also a factor in an ongoing debate about possible health risks of RF energy from communications systems. The problem is not whether effects exist (they surely do) but to understand their nature and anticipate the exposure conditions that will elicit them.

This paper reviews interactions of electromagnetic fields with biological systems, focusing on the relation between external and internal field strengths and mechanisms of in-

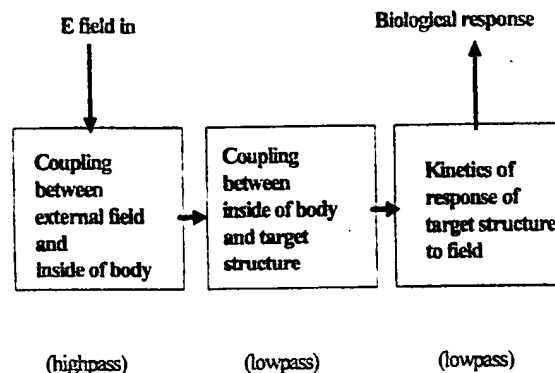


Fig. 1. Schematic showing different levels of field-tissue interaction. For a discussion of cutoff frequencies, see the text.

teraction. These two subjects are seldom discussed together. However, they are closely related, in that the field is typically specified in the air outside the body, whereas the field strength in tissue is the important dosimetric quantity. Most of the discussion concerns RF fields (3 kHz–300 GHz) but some discussion applies to pulsed fields with a broad spectrum, possibly including a dc component.

This paper reviews simple models that give insight into the orders of magnitude of phenomena, particularly as they relate to pulsed fields of high peak power but low duty cycle. Extensive reviews are available on dosimetry [3] and bioeffects and mechanisms of interaction [4]; see also the excellent but somewhat dated monograph [5]. The literature on biological effects of high-peak-low-average power RF pulses is sparse, however.

The interaction between RF energy and biological systems is a problem at three levels (Fig. 1). The first (macrodosimetry) concerns the relation between external fields and the resulting fields induced within the body on distance scales of centimeters or more. The second (microdosimetry) is the assessment of induced fields at the level of cellular or subcellular structures. The third is determining the biological response, if any, to the local field. Time or frequency enters at each level through the electromagnetic properties of the body (which are frequency-dependent) and the kinetics of the biological response.

## II. ELECTRICAL PROPERTIES OF TISSUE

The bulk electrical properties of tissue have been reviewed elsewhere [6]; for a recent compilation of data see [7]. The bulk

Manuscript received May 28, 1999; revised October 12, 1999.

The author is with the Department of Bioengineering, University of Pennsylvania, Philadelphia, PA 19104-6392 USA (e-mail: kfoster@seas.upenn.edu).

Publisher Item Identifier S 0093-3813(00)00734-7.

TABLE II  
THRESHOLD FIELD STRENGTHS AND RELAXATION FREQUENCY FOR  
SEVERAL MOLECULES.

| Molecule   | Dipole Moment $\mu$<br>(Debye) | Relaxation<br>Frequency | $E_0$ V/m      |
|------------|--------------------------------|-------------------------|----------------|
| Water      | 1.8                            | 20 GHz                  | $7 \cdot 10^8$ |
| Hemoglobin | 170                            | ca. 1 MHz               | $7 \cdot 10^9$ |
| DNA        | ~ 100,000 (varies)             | < 1 kHz                 | > 10,000       |

medium, some of them toxic [33]. Electrode impedance properties are strongly nonlinear, and rectification or generation of harmonics can occur. Electrode effects are an obvious potential cause of effects (or artifacts, depending on one's perspective) in studies in which RF fields are applied directly to biological preparations via electrodes.

The mechanisms described above are well established and noncontroversial. In addition, the scientific literature abounds with proposals for mechanisms, sometimes by highly respected physicists, for biological effects of RF energy at low exposure levels. This includes a theory for resonance-type effects reported from millimeter waves [34] or proposed mechanisms for biological damage from ultrawide-band pulses [35]. Many of these theories are experimentally unsupported, not accompanied by quantitative estimates of response times and thresholds, or can be challenged on obvious theoretical grounds [36] and they remain unpersuasive and controversial.

## VI. THE "MECHANISMS PARADOX"

As the above discussion shows, there are many mechanisms, both linear and nonlinear, thermal and nonthermal, by which RF or broadband electric fields can interact with biological materials. But careful analysis, that properly accounts for the strength of the interaction and dissipative effects, leads to high anticipated thresholds for producing observable effects. This arises in part from the nature of the coupling of external fields to the body, and in part from the strength of the interaction and the kinetics of response.

Indeed, the (very limited) studies to date have failed to disclose striking effects in animals exposed to ultrawide-band or EMP pulses (e.g., [37]–[39]), with field strengths (measured outside the body) of the order of tens of kV/m (ultrawide-band pulses) to hundreds of kV/m (EMP). The studies (e.g., by Schoenbach et al., [28]) that did report clear-cut effects utilized much stronger fields, applied directly to the preparation. Ultrawide-band and EMP pulses are clearly far more effective in damaging electronics (one of the purposes for which the technologies were developed) than in damaging biological cells. None of the considerations presented above suggest the possibility of nonthermal effects from the much weaker fields used in communications systems.

Paradoxically, many effects, sometimes at low exposure levels, of RF energy have been reported in the literature that clearly are not explicable in terms of the biophysical mechanisms discussed above. For example, many therapeutic effects of millimeter waves have been reported by investigators in the former Soviet Union. Many of these effects involve low

exposure levels ( $<0.1 \text{ W/m}^2$ ), at frequencies where the energy barely penetrates the (dead) outer layers of the skin [40], [41].

This paradox might be resolved in two ways. On the one hand, biophysical theory is surely not complete, and one can take for granted that interesting new mechanisms of interaction will be discovered. On the other hand, the experimental evidence is frequently unclear. Many studies that report effects are exploratory in nature, or subject to technical criticism, or the effects are close to the limits of statistical detection. Many reported effects find conventional explanations or simply disappear when followup studies are conducted under better controlled conditions [42]. It is the continued interplay of theory and experiment that creates reliable knowledge, and this has not even begun for many reported bioeffects. Given sufficient field strengths, however, there is no question that a range of effects will be produced. The issue then is to make productive use of them.

## ACKNOWLEDGMENT

The author thanks A. Pakhomov, H. Schwan, and two anonymous referees for helpful comments and suggestions about earlier drafts of this manuscript.

## REFERENCES

- [1] *EMF Database*. Philadelphia, PA: Information Ventures, Inc., 1999.
- [2] Y. A. Andreev, Y. I. Buyanov, V. A. Vizir, A. M. Efremov, V. B. Zorin, B. M. Kovalchuk, V. I. Koshelev, and K. N. Sukhushin, "A high-power ultrawideband electromagnetic pulse generator," *Instrum. Exp. Tech.*, vol. 40, no. 5, pp. 651–655, 1997.
- [3] C. H. Durney, H. Massoudi, and M. F. Iskander, *Radiofrequency Radiation Dosimetry Handbook*. USAF/SAM, Brooks Air Force Base, TX. [Online]. Available: <http://www.brooks.af.mil/al/oe/oer/handbook/cover.htm>
- [4] C. Polk and E. Postow, *Handbook of Biological Effects of Electromagnetic Fields*, 2nd ed. Boca Raton, FL: CRC Press, 1996.
- [5] S. M. Michaelson and J. C. Lin, *Biological Effects and Health Implications of Radiofrequency Radiation*. New York: Plenum, 1987.
- [6] K. R. Foster and H. P. Schwan, "Dielectric properties of tissues—A review," in *Handbook of Biological Effects of Electromagnetic Radiation*, 2nd ed., C. Polk and E. Postow, Eds. Boca Raton, FL: CRC Press, 1995, pp. 26–102.
- [7] S. Gabriel S, R. W. Lau, and C. Gabriel, "The dielectric properties of biological tissues. 2. Measurements in the frequency range 10 Hz to 2 GHz," *Physics in Medicine and Biology*, vol. 41, no. 11, pp. 2251–2269, 1996.
- [8] H. N. Kritikos and H. P. Schwan, "The distribution of heating potential inside lossy spheres," *IEEE Trans. Bio-Med. Eng.*, vol. BME-22, pp. 457–463, 1975.
- [9] A. W. Guy, "A note on EMP safety hazards," *IEEE Trans. Bio-Med. Eng.*, vol. BME-22, no. 6, pp. 464–467, 1975.
- [10] K. Moten, C. H. Durney, and T. G. Stockham, Jr., "Electromagnetic pulsed-wave radiation in spherical models of dispersive biological substances," *Bioelectromagnetics*, vol. 12, no. 6, pp. 319–333, 1991.
- [11] T. B. Jones, *Electromechanics of Particles*. Cambridge, U.K.: Cambridge Univ. Press, 1995, p. 113.
- [12] R. K. Adair, "Ultrashort microwave signals: A didactic discussion," *Aviat. Space Environ. Med.*, vol. 66, no. 8, pp. 792–794, 1995.
- [13] P. D. Smith and K. E. Oughstun, "Electromagnetic energy dissipation and propagation of an ultrawideband plane wave pulse in a causally dispersive dielectric," *Radio Sci.*, vol. 33, no. 6, pp. 1489–1504, 1998.
- [14] J.-Y. Chen and O. P. Gandhi, "Currents induced in an anatomically based model of a human for exposure to vertically polarized electromagnetic pulses," *IEEE Trans. Microwave Theory Tech.*, vol. 39, pp. 31–39, Jan 1991.
- [15] A. W. Guy, "Measured body to ground current and thermal consequences for human subjects exposed to 3.68 MHz to 144.5 MHz radiofrequency fields," in *Meeting Abstr. Bioelectromagnetics Soc.*, 9th Annu. Meeting, Portland, OR, June 21–25, 1987, p. 31.



at 5–120 GHz has given data on the double helix. We find that in the range of electrostatic-like forces, forces of some 40 base pairs are significant for B-conformation. When using assumptions concerning the dielectric constant, changing the dielectric constant giving rise to the long-range forces have disappeared, long-range forces formation as well. The effect concerned, extends over 30

$\nu$ -lying vibrational modes. The lowest lying optical mode is at about  $5\text{ cm}^{-1}$  in B. It is not greatly changed, however, when moving in opposite directions. For perturbations, which induce a change.<sup>12</sup>

tional modes has been taken into consideration. Only the bending

The inclusion of the effect is elsewhere.

NIH Grant GM24443, NSF Grant DMR81-13361, F33615-78-0617.

77) *Biopolymers* 16, 2481–2490.  
13, 2505–2526.

7) *Conformation of Biopolymers*,  
pp. 83–105.

*Biopolymers* 8, 475–488.

K. & Rupprecht, A. (1979) *Colloid*

39, 339–340.

sity.

0, 472–485.

$\nu$ -Hill, New York.

Chemical Properties of Nucleic  
91–145.

7) *Biopolymers* 16, 2491–2506.

16, 956–982.

## Calculated Microwave Absorption of Double-Helical B-Conformation Poly(dG)·Poly(dC)

M. KOHLI, W. N. MEI, E. W. PROHOFSKY, and L. L. VAN ZANDT,  
*Department of Physics, Purdue University, West Lafayette, Indiana 47907*

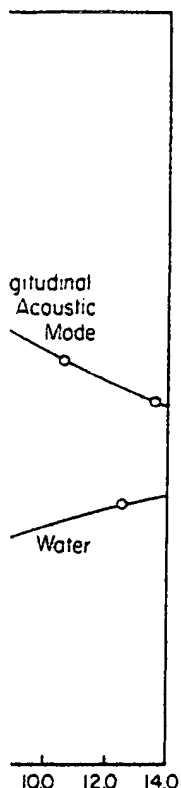
### Synopsis

We have estimated the absorption of microwave radiation by the four acoustic modes of poly(dG)·poly(dC) in B conformation. The eigenvectors used in this calculation are those obtained from a refined normal coordinate analysis by fitting the velocity of the longitudinal acoustic mode to that observed by Brillouin scattering. The acoustic modes couple to the radiation field when translational invariance is broken such as for finite segments of helix and as may be the case *in vivo*. Calculations for various helix lengths show that the estimated absorption is greater than that of water by at least two to three orders of magnitude in some cases.

### INTRODUCTION

Many researchers have reported observations of biological effects arising from microwave illumination. Much controversy exists as to whether all of the observed effects are due to microwave heating. There are reports of resonant, as distinct from thermal, effects.<sup>1</sup> Such resonant effects would likely arise from a resonant absorption by some part of a biologically active molecule. In our studies of the vibrational modes of DNA, we find internal vibrational modes present in the double helix at frequencies in the microwave range. In this paper we calculate the absorption of such modes in the microwave frequency range for the duplex homopolymer poly(dG)·poly(dC) in the B conformation. The absorption is based on the local electromagnetic field present at the macromolecule. The interaction with the field is via an oscillating dipole associated with the vibrational modes. This is calculated from our vibrational displacement eigenvectors and a rigid ion model of fixed net charge per atom as calculated by Renugopalakrishnan et al.<sup>2</sup>

The vibrational modes in the microwave frequency range are acoustic modes. The longitudinal acoustic branch has been observed in DNA fibers by Maret et al.<sup>3</sup> using a 5-pass Fabrey Perot in a Brillouin scattering experiment. In the preceding paper,<sup>4</sup> we have discussed the manner in which we have used the Brillouin scattering results and many Raman scattering and ir-absorption observations to refine a calculated model of the acoustic



Frequency for the longitudinal acoustic wave region (0 ~ 14 GHz) for a chain. The longitudinal acoustic mode has an absorption magnitude in this frequency range. The curves represent a comparison of the cross sections below 2.5

cannot affect the result by more than 1% in this same frequency range.

The values for water come from experimental observations.<sup>9</sup> The values for the DNA helix are calculated for a mass of water comparable to the DNA helix. The curves represent a comparison of the cross sections below 2.5

multiple to an  $E$  field polarized perpendicular to a transverse polarized field. The values for water do not affect the result over most of the band. We have calculated the dipole moment for the DNA helix. We have, however,

used the dispersion curve corrected for water effects in determining the frequency of the absorption. For values of  $\theta$  that are close to  $\psi$ , the two branches of the dispersion curve that originate at  $\theta = \psi$  will be symmetrical. Therefore, for the same  $(\theta - \psi)$  differences above and below  $\psi$ , the frequencies will be the same. The eigenvectors corresponding to these values of  $\theta$  do not differ significantly; therefore, in our estimate of the absorption cross section, we have a sum over the two frequencies originating from the portions of the dispersion curve for  $\theta$  values greater than and less than  $\psi$ . The envelope function of the absorption peaks calculated in this manner is shown as the curve labeled bending modes in Figs. 4 and 5.

## DISCUSSION

The calculations in the previous sections dealt with straight segments of DNA helix of various lengths. The results indicate that the helix is capable, under appropriate conditions, of absorbing microwave radiation which may be tuned to some segment of helix at a rate many orders of magnitude greater than that of an equivalent mass of water. The details of the absorption depend on certain geometrical factors such as effective segment length and helix orientation with respect to the field polarization. The actual absorption of DNA *in vivo* would depend in detail on the particular geometrical distribution of DNA and its orientation to the microwave field. *In vivo* DNA is made of very long segments, which are, however, folded in a very complex manner. A gently curving segment could support resonant acoustic modes matched to its entire length but only have some fraction of its length properly oriented so as to absorb in a given field. In this case one would expect some fraction of the absorption predicted for a straight, properly oriented segment. It is possible that some regions of chromosomes are so arranged as to be able to resonantly absorb radiation. If such absorption regions do occur, there are still a number of questions relating to the flow of absorbed energy from such regions which will be important in determining whether biologically significant "hot spots" can occur as a result of microwave irradiation.

This work was supported in part by FDA Grant FD00949 and Air Force Contract F33615-78-0-0617.

## References

1. Grundler, W. & Keilman, F. (1978) *Z. Naturforsch., Teil C* 33, 15-18.
2. Renugopalakrishnan, U., Lakshminarayanan, A. & Sasiesekharan, V. (1971) *Biopolymers* 10, 1159-1167.
3. Maret, G., Oldenbourg, R., Winterling, G., Dranfeld, K. & Ruprecht, A. (1979) *Colloid Polym. Sci.* 257, 1017-1020.
4. Mei, W. N., Kohli, M., Prohofsky, E. W. & Van Zandt, L. L. (1981) *Biopolymers* 20, 833-852.
5. Lu, K. C., Prohofsky, E. W. & Van Zandt, L. L. (1977) *Biopolymers* 16, 2491-2506.

21. W. J. BAIR and R. C. THOMPSON, Plutonium: Biomedical research. *Science* **183**, 715-722 (1974).
22. F. F. HAHN and B. B. BOECKER, Tumors of the tracheobronchial lymph nodes in Beagle dogs after inhalation of a relatively insoluble form of cerium-144. In *Pulmonary Toxicology of Respirable Particles* (C. L. Sanders, F. T. Cross, G. E. Dagle, and J. A. Mahaffey, Eds.), pp. 591-600. U.S. Department of Energy Technical Information Center, Oak Ridge, TN, 1980.
23. J. L. LEBEL, E. H. BULL, L. J. JOHNSON, and R. L. WATTERS, Lymphosarcoma associated with nodal concentration of plutonium in dogs: A preliminary report. *Am. J. Vet. Res.* **31**, 1513-1516 (1970).
24. G. E. DAGLE, R. W. BISTLINE, J. L. LEBEL, and R. L. WATTERS, Plutonium-induced wounds in Beagles. *Health Phys.* **47**, 73-84 (1984).
25. K. WEGENER, H. WESCH, Pathological changes of lymph nodes in Thorotrast patients: Pathoanatomical autoradiographical and quantitative investigations. *Environ. Res.* **18**, 245-255 (1980).
26. P. R. BEVINGTON, *Data Reduction and Error Analysis for the Physical Sciences*, McGraw-Hill, New York, 1969.

REVOLUTION RESEARCH **110**, 219-231 (1987)

## Microwave Effects on Plasmid DNA

JOSE-LUIS SAGRIPANT, MAYS L. SWICORD, AND CHRISTOPHER C. DAVIS<sup>1</sup>

*Center for Devices and Radiological Health, Food and Drug Administration, Molecular Biology Branch,  
5600 Fishers Lane, Rockville, Maryland 20857*

SAGRIPANT, J. L., SWICORD, M. L., AND DAVIS, C. C. Microwave Effects on Plasmid DNA. *Radiat. Res.* **110**, 219-231 (1987).

The exposure of purified plasmid DNA to microwave radiation at nonthermal levels in the frequency range from 2.00 to 8.75 GHz produces single- and double-strand breaks that are detected by agarose gel electrophoresis. Microwave-induced damage to DNA depends on the presence of small amounts of copper. This effect is dependent upon both the microwave power and the duration of the exposure. Cuprous, but not cupric, ions were able to mimic the effects produced by microwaves on DNA. © 1987 Academic Press, Inc.

## INTRODUCTION

Because microwave (MW) devices are in such widespread consumer, medical, commercial, industrial, and military use, where there is potential risk for human exposure to the radiation, multidisciplinary research has been conducted to delineate possible associated health hazards. Epidemiological reports have raised concern about carcinogenic or tumor-promoting properties associated with such nonionizing radiation (1, 2). *In vivo* as well as *in vitro* studies have identified changes in parameters which are usually linked to the development of cancer after exposure to low levels of MW (3, 4). On the other hand, MW at higher levels have been shown to retard tumor growth (5, 6). Chromosomal abnormalities, aberrations, and aneuploidy have been reported in cells and animals chronically exposed to nonthermal levels of MW (7, 8). Low levels of MW have also been demonstrated to alter immune competence and general hematopoietic function (9, 10). Léonard *et al.* (11) have concluded that most direct mutagenic, carcinogenic, and teratogenic effects reportedly caused by low-level microwave exposure may still have a thermal origin. However, they believe that microwaves may play a synergistic role in causing damage to DNA in the presence of antagonistic chemical agents. Nonetheless, the absence of a clear mechanism other than thermal heating for the interaction of MW with biological systems has made difficult the assessment of possible risks associated with low-level MW exposure.

In an attempt to identify any fundamental mechanism that could explain the MW bioeffects observed at nonthermal exposure levels, physical studies carried out in our laboratory have shown MW absorption by DNA molecules in aqueous solution (12). The MW absorption was dependent upon the size of the DNA molecule (13). DNA

<sup>1</sup> Electrical Engineering Department, University of Maryland, College Park, MD 20742.

tional coupler and the attenuation of the system components with calibrated power sensors, we could accurately relate the forward power at the antenna to the recorded power from the dual-directional coupler shown in Fig. 1. Under exposure conditions, the VSWR in the system was measured. These measurements were made at low power to avoid saturation effects and used minimal probe penetration in the slotted line. The fractional amount of forward power that is not reflected at the open antenna is then determined from the formula

$$T = 1 - [\tanh(r(\text{dB})/17.372)]^2,$$

where  $r(\text{dB})$  is the VSWR. The measured VSWR was insensitive to the volume of sample for sample volumes in the range 20–100  $\mu\text{l}$  and corresponded to  $T = 0.144 \pm 0.015$ . If all the forward power  $P$  at the antenna is assumed to be absorbed in a sample of mass  $M$  then a maximum SAR ( $\text{SAR}_{\text{max}}$ ) is determined from the formula

$$\text{SAR}_{\text{max}} = TP/M.$$

Since some of the power is lost by passing right through the sample, the actual SAR ( $\text{SAR}_{\text{true}}$ ) will be smaller than  $\text{SAR}_{\text{max}}$ .

To determine a minimum SAR ( $\text{SAR}_{\text{min}}$ ), a Hughes Model 1177H amplifier was placed after the generator in Fig. 1 to boost the power applied to the sample. With a Vitek Model 101 probe, the temperature rise  $\Delta T$  of the sample as a function of time  $t$  could then be measured.  $\text{SAR}_{\text{true}}$  will be greater than this because the thermal mass of the antenna, Vitek probe, and micro test tube reduces the observed  $\Delta T/\Delta t$ . The inserted volume of the probe in these experiments is about 2  $\mu\text{l}$ , so it is not the dominant thermal sink. We should point out that the Vitek probe was not immersed in the DNA samples during actual exposures and was used only during dosimetric calibrations. Under the conditions of our experiment, we measured  $\text{SAR}_{\text{max}} \sim 5\text{SAR}_{\text{min}}$ . Obviously,  $\text{SAR}_{\text{min}} < \text{SAR}_{\text{true}} < \text{SAR}_{\text{max}}$ .

During microwave exposure, the electric field at the surface of the antenna can be calculated from the forward and reflected powers, and the annular area,  $A$ , between the inner and outer conductors of the coax. The maximum surface field results when all the power is reflected. In this case, the field,  $E$ , associated with the forward traveling wave is related to the forward power,  $P_{\text{forward}}$ , as follows,

$$P_{\text{forward}} = AE^2/(2Z),$$

where  $Z$  is the characteristic impedance of the coaxial line, 50 ohm in this case. The maximum possible field at the antenna surface is

$$E_{\text{max}} = 2(2ZP_{\text{forward}}/A)^{1/2}.$$

For an annular area of  $6.0 \times 10^{-6} \text{ m}^2$  and a forward power of 0.28 mW (corresponding to 10 mW/g for 28  $\mu\text{l}$  of sample) the maximum surface field is about 136 V/m.

### Characterization of the DNA Sample

Plasmid pUC8.c2 DNA was analyzed by AGE under nondenaturing conditions. The DNA was incubated with various amounts of the restriction nuclease *Pst*I. This enzyme has a single cutting site in pUC8, which is the precursor of pUC8.c2 (17).

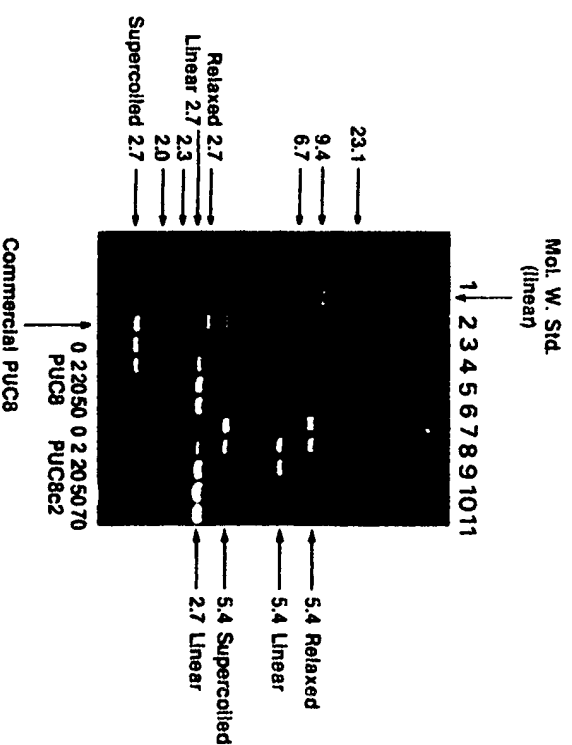


FIG. 2. Identification of species in the pUC8.c2 plasmid by restriction mapping with the *Pst*I enzyme. Plasmid DNA (10  $\mu\text{g}$ ) was digested with 0, 2, 20, 50, or 70 units of *Pst*I for 60 min at 19°C. Treated DNA was sampled on 1% agarose gel and electrophoresed 9 h at 80 V, 80 mA. After staining with ethidium bromide, photographs were made. Commercial pUC8 and pUC8 prepared in our laboratory and digested with 0, 2, 20, and 50 units of *Pst*I are included for comparison. A *Hind*III digest of  $\lambda$  phage DNA, showing the linear subunits 23.1, 9.4, 6.7, 2.3, and 2.0 kb long, is included as the molecular weight standard (Mol. W. Std.).

Low levels of enzyme present during short incubations produced partial digestion of plasmid DNA (Fig. 2, lanes 4 and 8). Further digestion resulted in total conversion into the linear form of the plasmid as a consequence of double-strand breaks. Complete digestion of pUC8.c2 yielded the 2.7-kb linear form identical to the one obtained by digestion of pUC8 (lanes 11 and 6, respectively), indicating that pUC8.c2 consists of two pUC8 genomes linked together. Comparison with molecular weight standards in lane 1 permits the corresponding structures to be assigned to the remaining bands.

### Effect of Microwaves on DNA

Since our previous work had indicated a maximum absorption of microwaves at 2.55 GHz (14), we exposed 10  $\mu\text{g}$  of plasmid DNA at this frequency for 20 min in 28  $\mu\text{l}$  of storage buffer, using the exposure system shown in Fig. 1. To avoid any systematic errors, the DNA was divided into identical samples and randomly assigned to the different treatments (MW exposed or sham exposed). The order of the treatments was also randomized. Subsequent analysis of exposed DNA by AGE showed increased amounts of relaxed circular and linear DNA after MW exposure. Figure 3 demonstrates that the relaxation of DNA is power dependent.

## Resonant Microwave Absorption by Dissolved DNA

L. L. Van Zandt

*Department of Physics, Purdue University, West Lafayette, Indiana 47907*

(Received 12 May 1986)

The anomalous microwave absorption resonances recently observed in aqueous solutions of DNA are explained in terms of a layered structure of water molecules around the polymer. At high frequencies the interactions with water become elastic instead of viscous.

PACS numbers: 87.15.-v, 33.20.Bx, 68.45.Kg

Aqueous solutions of oligopolymer DNA have been observed by Edwards, Davis, Saffer, and Swicord (EDSS)<sup>1</sup> to show structured absorption of microwave energy in the region of several gigahertz, characteristic of an ordered series of compressional normal-mode vibrations propagating on the polymer chain. Although simple hydrodynamic coupling of such vibrations to the surrounding solvent would preclude the existence of sharp resonances, the molecular nature of the solvent in the near neighborhood of the polymer and—paradoxically—the strong water-polymer interactions provide a means for effectively decoupling the polymer motion from the dissipation of the liquid. Recent measurements of DNA-water relaxation times suggest a range of numerical values for parametrization of the decoupling effect. The resulting predicted frequency dependence explains many of the smaller features of the EDSS experiment as well as the overall anomaly. A simple model gives a surprisingly complete account of the features of the data.

Figure 1 shows data of EDSS<sup>1</sup> on the absorption of microwaves by a dilute solution of DNA polymer. The dissolved material consists of plasmids, closed loops of bacterially grown material all having the same length, 5480 base pairs. The lower (dashed) curve is for as-grown material known to be strongly supercoiled; the upper (bold solid) curve shows absorption by the same plasmids after being nicked with a topoisomerase to relieve the supercoiling. In both cases, a featureless background of absorption has been subtracted before plotting.

The aspect that makes these data surprising and controversial is that there was strong reason to believe that no resonant structure could avoid heavy damping under the close coupling to the viscous solvent.<sup>2</sup> The frequency locations of the resonances are close to those expected for "organ pipe" modes of the polymer, longitudinal compressional standing waves.

The organ-pipe modes of DNA polymer were first observed by Maret, Oldenbourg, Winterling, and Dransfeld.<sup>3</sup> From this work and its subsequent confirmation by Lindsay, we know that the isolated chain supports well-defined resonances, but it had long been supposed that the effect of water coupling is to damp

all the molecular motion in thoroughly hydrated systems. Hence, the results of the calculations of Dorfman and Van Zandt<sup>2</sup> were not controversial nor even surprising.

In the third curve (light solid line) of Fig. 1, I show the results of a calculation of power absorption based on a simple model of a structured water-DNA interface. The choice for the lifetime parameter corresponds to that found by Tao, Lindsay, and Rupprecht<sup>4</sup> for fibers at 238 K. This does *not* correspond with the EDSS experiments, which were done in solutions at room temperature. (Details of the solvent dynamics have been relegated to a longer exposition elsewhere.<sup>5</sup> While a possible discrepancy in the lifetime remains, it is clear that this model successfully reproduces many of the details of the experiments, as well as the overall anomalous resonant structure.

The model is based on the so-called "V structure" of water<sup>6</sup> in which the dominant source of viscosity is a

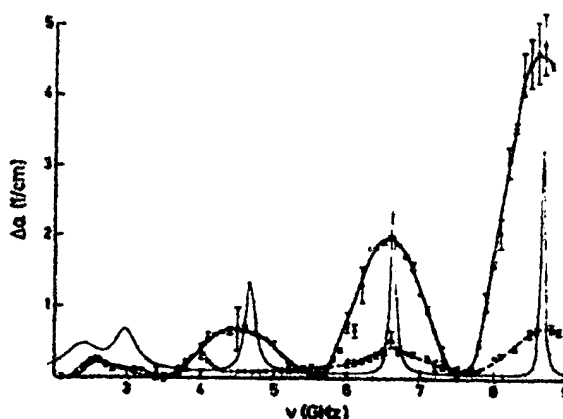


FIG. 1. Absorption spectrum of dissolved DNA plasmids in water. Compared with previously published data, these plasmids have been attacked by topoisomerase with consequent relaxation of much of their supercoiling. Overlaying is the theoretical curve (light solid line) of microwave power absorption by weakly supercoiled DNA plasmids of 5480-base-pair lengths. The curve is based on the model described in the text. The value of  $\tau_1$  is  $3 \times 10^{-10}$  sec. The value used for  $\Gamma_{dc}$  is  $0.414 \times 10^{-3}$  N·sec/m.

## Why Structured Water Causes Sharp Absorption by DNA at Microwave Frequencies\*

L.L. Van Zandt  
Purdue University  
Department of Physics  
W. Lafayette, Indiana 47907

### *Abstract*

Aqueous solutions of oligopolymer DNA have been observed by G.S. Edwards, C.C. Davis, M.L. Swicord and J.D. Saffer, *Phys. Rev. Lett.* 53, 1284 (1984) to show structured absorption of microwave energy in the region of several gigahertz, characteristic of an ordered series of compressional normal mode vibrations propagating on the polymer chain. Although hydrodynamic coupling of such vibrations to the surrounding solvent would preclude the existence of sharp resonances, the molecular nature of the solvent in the near neighborhood of the polymer and - paradoxically- the strong water/polymer interactions provide a means for effectively decoupling the polymer motion from the dissipation of the liquid. Recent measurements of DNA/water relaxation times allow estimating numerical values in a parameterization of the decoupling effect. The resulting predicted frequency dependence explains many of the smaller features of Edwards' experiment as well as the overall anomaly. A simple model gives a surprisingly complete account of the features of the data using only values determined from other experiments.

### *Introduction*

Edwards, Davis, Swicord and Saffer, (1) (EDSS), have recently reported the observation of resonant structure in the microwave absorption spectrum of dilute aqueous solutions of DNA double helical polymer chains of carefully controlled lengths. Earlier theoretical studies had analyzed the mechanics of DNA in terms of vibrational acoustic normal modes (2). The locations of the observed resonances correspond very well to the frequencies of compressional waves on drier DNA chains as observed by Lindsay (3). The known lengths of the polymer chains combined with the measured velocity of compressional sound on DNA yield the frequencies of the EDSS results. This numerical coincidence suggests that the observed structure arises in fact from resonant absorption by long chain compressional waves.

A simple model of DNA/solvent interaction showed that any such resonant structure should be strongly overdamped by the viscosity of the solvent (4). In comparison to a continuum hydrodynamic theory of the surrounding solvent, the EDSS measurements are anomalous by about 2 orders of magnitude. We have recently

shown (5) that if an extra degree of freedom be introduced in the polymer motion relative to the solvent, only a small amplitude of excitation of the extra coordinate suffices to give resonance of the type observed. The extra coordinate was introduced in (5) as an ad hoc extra parameter in the polymer/solvent boundary relation, but without any attempt at justification; it was merely a way of parametrizing the necessary condition for obtaining resonant behavior to match the experiment. In this discussion, we show how the extra coordinate arises naturally from the structure of molecular water near the polymer.

We are specifically concerned with the consequences of the discrete molecular nature of the water at the interface with the polymer. One way to investigate this as a theoretical question would be through the use of a full molecular dynamics computer simulation of the polymer/water system. Attempts which have been made so far along those lines (6) have not included sufficiently many water molecules in the model to shed any light on the problem of truly dissolved DNA. These investigations rather probe the nature of the first hydration shell. Likewise, Monte Carlo calculations (7) can not tell us about the dynamical behavior of this system, even though they have yielded very interesting results on the nature of the structured interface.

Both as a way of avoiding the computational overhead of these enormous calculations and also to obtain more insight into the basic physics of the situation, we sought to construct a model of the molecular water/polymer which would retain the essential features of the system but no more. This approach can be very useful for illuminating aspects of a physical system a posteriori and for detailing how these aspects may respond to changing system variables like temperature and frequency. New, unexpected effects are unlikely to be predicted by modeling, of course. The model we use here proves to be very successful in explaining the data despite its severe simplicity.

#### *The Water Model*

DNA is a strongly charged molecular chain. In the B form appropriate to aqueous solution each base pair on net holds  $-2e$  in charge, and the base pairs are separated by  $3.4\text{\AA}$ . A cloud of counterions, almost exclusively cations at close range, surrounds the chain. Overall charge neutrality is achieved at as short a range as 5 to  $10\text{\AA}$  out from the polymer radius.

Within the neutralization radius, the highly polar water molecules are subject to strong electric fields. The water becomes highly structured and layered.

In any liquid, the distribution of molecules as a function of distance from any particular one of them shows a strong division into near neighbors, next near neighbors, etc. blending finally into a homogeneous average density far away. X-ray analysis typically reveals this particle-particle density correlation. Monte Carlo calculations (7) show corresponding structure around DNA polymer and even more sharply defined layering around isolated constituent molecular moieties. We will model the dissolved DNA system in such a way as to build in this layered structure to the surrounding liquid.

U —  
S —

Figure 1: Car  
thin slice of t

In Figure 1  
of water. T  
molecule s  
density of l  
longitudin  
than the ra  
we proceed  
one stops, t  
pagation o  
speed of so  
a minor cc  
dynamics i

The most in  
and between  
case of the  
over each o  
of transmis  
we would b

where  $\eta$  is t  
the area ov  
we get

$\delta v$  is the di  
thickness c  
ing blocks  
continuum

There are t

me derivatives  
to this system.

[9]

al elasticity of  
oring constant  
to produce a  
on is a small

base pair and  
the interbase  
act across the  
tion of a slice  
aces of a slice  
avelength dis-  
ars as the elas-  
e place of  $\kappa$  in

water layer. Let  
isturbance be  
e velocities of

[10]

that  $\gamma$  plays in  
equations.

racts with the  
ea A, we take

[11]

ng coefficient

$$\gamma = (2\pi r a) \eta \frac{dv/dr}{v} \quad [12]$$

It is instructive at this point to consider how the calculation would go without the second mass  $m_2$ . Let the slice, the first mass, be coupled directly to the water with the same damping constant as the second mass is coupled to its neighbor. This is actually the calculation of Dorfman and Van Zandt from reference (4). Dropping the second equation in [8] and coupling the slice directly to the water yields

$$z = \frac{e}{m_1(\omega_0^2 - \omega^2) + i\gamma\omega} \quad [13]$$

The introduction of the intermediate water layer has approximately changed  $\gamma$  into  $\Gamma/\gamma$  so far as the motion of the DNA is concerned. The new damping factor in the DNA equation of motion is thus related to the simple hydrodynamic one by a factor of  $\eta_0^2/\eta$  where  $\eta_0$  is the viscosity we would obtain if the force between water layers were replaced by that operative between the DNA and the first layer.

But we have already seen that this later force is characterized by an effective time at least an order of magnitude longer than the bulk water one. If we assume that the strength of the coupling is the same in the two cases, that only the time constant is changed, the frequency dependent correction factor on the DNA damping - compared to the zero frequency case of reference (4) is

$$\eta'/\eta = (1 - i\omega\tau_2) / (1 - i\omega\tau_1)^2 \quad [14]$$

Because  $\tau_1$  is so much greater than  $\tau_2$ , the effective damping rate is greatly reduced.

To do a somewhat better job of this calculation, we should take account of the fact that  $\frac{dv}{dr}$  as it appears in equation [9] is not the same at the DNA interface as between the two hydration layers. To find  $dv/dr$  we should, strictly speaking, solve the coupled problems of continuum liquid motion, electromagnetic field equations, and DNA slice equation of motion. This would give us a value for  $\frac{dv}{dr}$  at a distance corresponding to one layer from the interface. This value then yields the damping coefficient for the first water hydration shell. The process of needs must be carried out self consistently. This process has been done and will be reported in a more detailed account elsewhere (8).

#### Implications of the Model

Equation [9] describes the local motion of a portion of the DNA helix assuming excitation of a single mode of resonant frequency  $\omega_0$ . On a length of helix  $L$  many harmonics of differing wavelengths could propagate. The motion would consist of a series of terms proportional to  $e^{ikz}$  with  $k = n\pi/L$  and a corresponding  $\omega_0 = c k$  for each mode. The complete absorption spectrum should show a resonance at each allowed  $k$ .



## Theory of the Anomalous Resonant Absorption of DNA at Microwave Frequencies<sup>\*</sup>

L.L. Van Zandt & M.E. Davis  
Purdue University  
Department of Physics  
W. Lafayette, Indiana 47907

### *Abstract*

Aqueous solutions of oligopolymer DNA have been observed by Edwards, Davis, Swicord & Saffer to show structured absorption of microwave energy in the region of several gigahertz characteristic of an ordered series of compressional normal mode vibrations propagating on the polymer chain. Hydrodynamic coupling of such vibrations to the surrounding solvent would preclude the existence of sharp resonances. The inclusion of electromagnetic interactions with surrounding counter ions yields a richer space of possibilities for complex behavior of the combined system. A well defined resonant absorption peak appears when the molecular motion and the nearby solvent motion are even slightly decoupled. The microwave electric fields in the vicinity of the molecule provide a mechanism for such a decoupling not present for the case of electrically neutral solvent.

### *Introduction*

G.S. Edwards, C.C. Davis, M.L. Swicord and J. Saffer (1) (EDSS) have recently reported the observation of sharp resonances in the microwave absorption spectrum of dilute aqueous solutions of DNA double helical polymer chains of carefully controlled lengths. Earlier theoretical studies had analyzed the mechanics of DNA in terms of vibrational acoustic normal modes (2). The locations of the observed resonances correspond very well to the frequencies of compressional waves on drier DNA chains as observed by Lindsay (3). The known lengths of the polymer chains combined with the measured velocity of compressional sound on DNA yield the frequencies of the EDSS results. This numerical coincidence suggests that the observed structure arises in fact from resonant absorption by long chain compressional waves.

This interpretation of the EDSS results has been criticized from two directions. First, experimentally, the measurements are extremely difficult, the observed structural features are very weak—not much above the noise level to be expected in these systems, and the apparatus may be susceptible to the generation of similarly structured peaks unrelated to the samples. Second, theoretically, Dorfman and Van Zandt (4) have calculated the damping of exactly these modes to be expected to arise from coupling of the mechanical motion of the DNA polymer to the surrounding

<sup>\*</sup>Work performed under ONR Contract #N840401

solvent bath. Such damping was found to be too large by approximately two orders of magnitude to allow for a well defined identity of these sorts of oscillations.

The purpose of this discussion is to show how the theoretical criticism could be circumvented by a different model of the molecule-liquid interface and what properties in a revised model of this interaction would be needed to explain the observations. It should be mentioned that the Boussinesq soliton theory as applied by Scott & Jensen (5) to this problem shares a number of qualitative features similar to the experiments; however, detailed numerical comparison (6) of the best current values of DNA parameters and the Scott & Jensen expressions fails of a satisfactory resolution of the anomalies by about 3 orders of magnitude.

In the calculation of Dorfman and Van Zandt, (DVZ), it was assumed that the solvent strongly wetted the molecular surface. This perfect "stick" boundary condition is in keeping with the strongly hydrophilic nature of the exposed backbones of the DNA helices. In the DVZ model, to reduce the damping effect of the water by a sufficient amount to allow for well defined resonances to appear, it would be necessary to decouple the motion of the molecule and the solvent at the interface almost entirely, leaving only a remnant of the interaction. One would need to pass almost to the opposite extreme—perfect "slip" boundary conditions—before sharp resonances would become possible. Since the closest layers of water molecules are known (7) to bond rather tightly to the molecule, it is very difficult to see how such a slipping could ever come about in the context of the DVZ model.

The present model incorporates counterion currents in a realistic way along with a proper dynamical treatment of the electromagnetic fields. The counterions in the present discussion add a new feature: the solvent is electrically active and so responds to the electric fields, both DC and microwave, in the molecule vicinity. This addition has several important consequences. First, the electrical behavior of the solvent modifies the nature of the microwave electric field near the molecule, decreasing it somewhat. But more importantly, the presence of charged ions in the water provides a means whereby the electric field can interact directly with the solvent in addition to the indirect effect of first driving the molecule that subsequently mechanically couples to the liquid.

It is important to note that the negatively charged DNA molecular ion attracts to itself a cloud of positively charged counterions. The electric forces applied to the molecule and the near solvent are hence oppositely directed. Thus compared to the neutral solvent model of Dorfman and Van Zandt, the model presented here includes an additional, strong shearing force between molecule and solvent directly at the interface. The argument for the perfect "stick" boundary condition is thereby considerably weakened.

Furthermore, the existence of a direct field-to-solvent interaction means that the liquid behavior may be (and is) considerably different than if it were simply a response to the motion of the molecule. It even becomes more appropriate to

regard  
than th

A final  
of two  
molec  
solvent  
livered  
happy i

If perfe  
from th  
trum. I  
resonai

Dorfma  
solvent  
cule. T  
assume  
have th  
bounda  
and liq  
yield a  
as a wh

The lin  
should  
the the  
ditions  
surface  
fere wit  
a featur

If the  
resonar  
slipping  
"stick"  
length,  
the "slip  
and the  
electric  
disparit  
dissipat  
electric  
goes th  
contrib

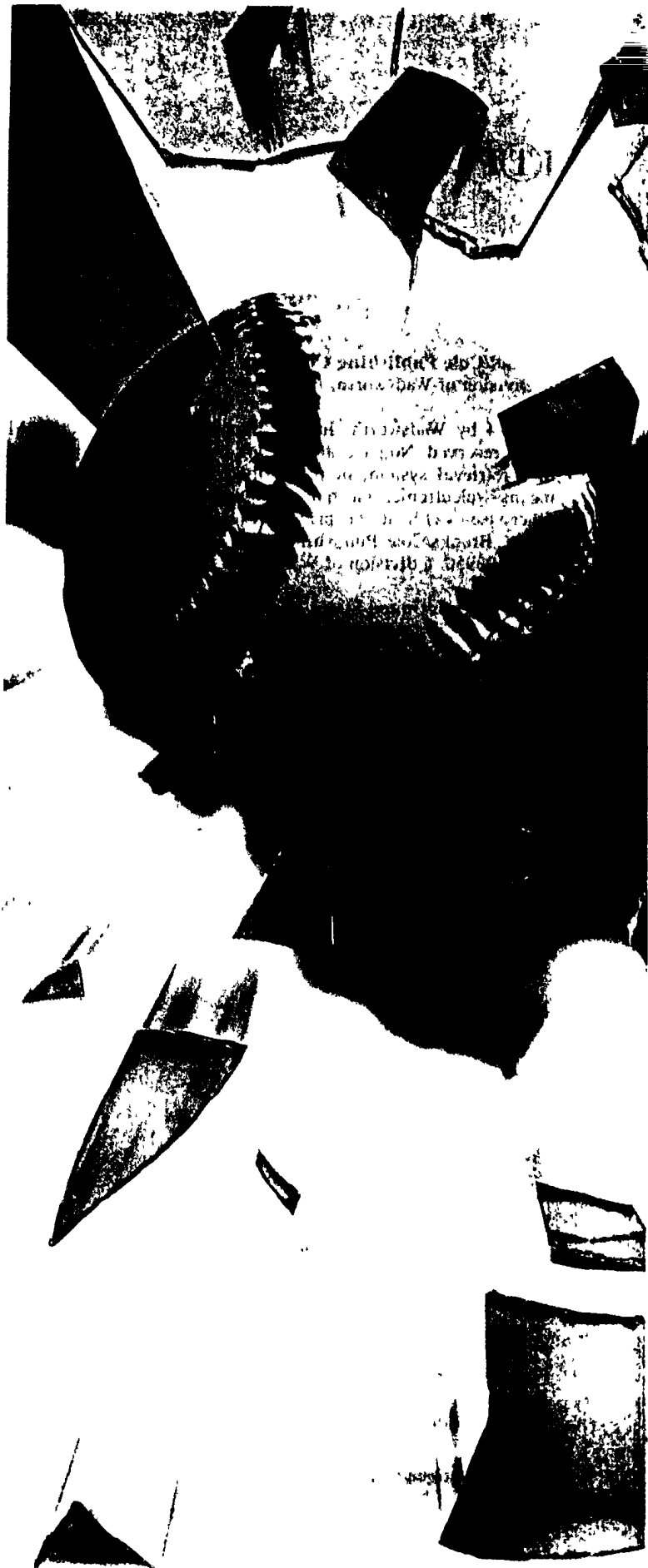
# VOLUME ONE **PHYSICS**

**EUGENE HECHT**

Adelphi University



Brooks/Cole Publishing Company  
Pacific Grove, California



**Brooks/Cole Publishing Company**  
A Division of Wadsworth, Inc.

© 1994 by Wadsworth, Inc., Belmont, California 94002. All rights reserved. No part of this book may be reproduced, stored in a retrieval system, or transcribed, in any form or by any means—electronic, mechanical, photocopying, recording, or otherwise—without the prior written permission of the publisher, Brooks/Cole Publishing Company, Pacific Grove, California 93950, a division of Wadsworth, Inc.

Printed in the United States of America

10 9 8 7 6 5 4 3 2

The Library of Congress has cataloged the single-volume edition as follows:

Hecht, Eugene.

Physics / Eugene Hecht.

p. cm.

Includes index.

ISBN 0-534-09114-8

1. Physics. I. Title.

QC23.H3917 1994

530—dc20

93-43106  
CIP

ISBN 0-534-09130-X

Sponsoring Editor: *Lisa J. Moller*  
Project Development Editor: *Suzanne Ewing*  
Editorial Assistant: *Beth Wilbur*  
Production Editor: *Marjorie Z. Sanders*  
Production Assistant: *Tessa A. McGlasson*  
Manuscript Editor: *Stuart Kenter*  
Permissions Editor: *May Clark*  
Interior and Cover Design: *E. Kelly Shoemaker*  
Cover Photo: *Tom Skrivan*  
Art Coordinator: *Susan Haberkorn*  
Interior Illustration: *Precision Graphics, Carl Brown,*  
*LM Graphics, Matrix Communications*  
Photo Coordination and Digital Photo Design: *Larry Molmud*  
Photo Researcher: *Stuart Kenter*  
Typesetting: *Beacon Graphics*  
Cover Printing: *Phoenix Color Corporation*  
Printing and Binding: *R.R. Donnelley & Sons Company/Willard*  
Credits continue on p. C1.

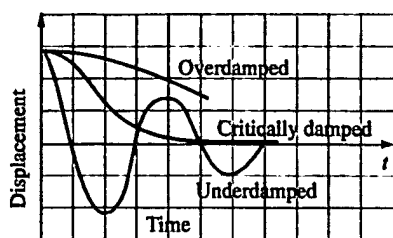


**Figure 12.22** When a damped oscillating system experiences still more friction, it will stop vibrating and the motion will gradually decay. The system is then overdamped. When the motion decays as quickly as possible, the system is critically damped.

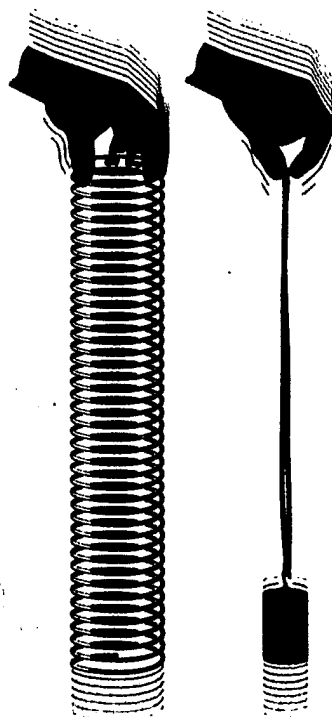


**Figure 12.23** By moving up and down, the hand pumps energy into the system, forcing it to oscillate at the driving frequency.

sandwiches of lead plates and spongy absorbent foam. There are space satellites that contain little carts that ride back and forth along tracks, set into motion by any inadvertent wobbling of the vehicle. Eventually the wobble is damped out and the carts come to rest—the kinetic energy of the satellite having been converted into thermal energy via friction in the carts. The World Trade Center in New York contains viscoelastic dampers: large plates coated with a sticky polymer that drag across one another whenever the towers sway in the wind. They convert troublesome shear energy into harmless thermal energy.

### Forced Oscillation and Resonance

One way to sustain the oscillations of a system suffering damping is to periodically pump in energy via a force that does positive work on the system. Pushing a playground swing can keep it going indefinitely, despite friction. When mom pushes, it's best done after junior has reached the peak of the swing and is moving away from her so she does positive work on the system ( $F$  and  $\Delta s$  are parallel). Energy is efficiently transferred to the system when it is pumped in in step with the natural oscillation. Accordingly, mom can push at the natural frequency, or miss a beat and push at one-half the natural frequency, or miss two and push at one-third the natural frequency, and so on.

The application of an *external alternating* driving force to a system capable of vibrating produces **forced oscillation**. The specific physical causes are many. Pulsations of pressure in lines carrying fluids will cause vibrations—some houses have “singing” plumbing, and refrigerators and air conditioners often buzz.

Forced oscillation is easily seen with either a Slinky or a mass on a long elastic band (Fig. 12.23). Displace either and let it loose to oscillate at its natural frequency ( $f_0$ ), which for the Slinky will be around 1 Hz. That done, stop the oscillation and now move your supporting hand up and down with a small amplitude ( $\approx 2$  cm) at a very low frequency ( $f \approx 0.3$  Hz,  $T \approx 3.0$  s), thereby driving the elastic system into motion. The Slinky will follow your hand (the driver), moving upward when your hand moves up, and downward when it moves down; that is, the Slinky will oscillate in-phase with the driver. Moreover, it will oscillate at the same frequency ( $f$ ) as the driver but with a relatively small amplitude, not much different from that of your hand. Little energy is transferred from the driver to the Slinky as the process continues.

Similar behavior occurs when the driving frequency is much greater than the natural frequency ( $f \gg f_0$ ) except now the two will be nearly  $180^\circ$  out-of-phase—when your hand goes down, the Slinky will move up, and vice versa. One thing will become obvious when you further vary the driving frequency—as  $f$  approaches the natural frequency of the system, the resulting oscillation will dramatically increase in amplitude (Fig. 12.24). The vibrational amplitude will reach a maximum when  $f = f_0$ , a condition known as **resonance**. At that special driving frequency, which is also known as the **resonant frequency**, energy is most efficiently transferred to the system, whether it's a hand-pumped Slinky, a windblown skyscraper, or a human internal organ set into vibration by the overamplified tumult of a rock band. It seems that every material object can oscillate somehow. As a rule, a body can bend, twist, and elongate in several different ways, displaying one or more natural frequencies at which it can resonate. Similarly, a composite object, such as a bus, in addition to vibrating as a whole, will have lots of resonant modes for its various parts—windows, doors, seats, and so on.

At resonance, most of the small amount of energy available during each cycle is stored in both the elastic medium and the moving mass; none is returned to the



An earthquake caused the collapse of the double-decked Nimitz Freeway in Oakland, California, in 1989. This portion of the highway rests on fine-grained sediments and mud that transmitted frequencies of around 2 Hz. This value is close to the natural frequency of the highway, which experienced violent resonant vibrations. Fifty-three cars were crushed when the supports for the top deck gave way.

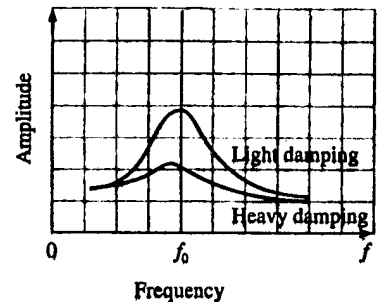


**Figure 12.24** The less damping there is, the sharper and taller is the amplitude versus frequency curve. The system responds more selectively to being driven at its resonant frequency.

driver, though a bit is invariably lost to friction. The less damping there is, the sharper and taller is the curve (Fig. 12.24), the greater the resulting amplitude of the vibration and the nearer that peak is to the resonant frequency. In a lightly damped system such as a bell, gong, or turbine blade, the stresses occurring at resonance can be upwards of 300 times larger than those resulting from the same applied force acting at a much different frequency.

The phenomenon of resonance is one of the most important in all of physics. It is at the heart of a tremendous diversity of occurrences from the atomic absorption and emission of light to the tuning of a TV set, from the swaying of bridges to the rattling of china cabinets when a low-flying plane passes overhead.

**Example 12.6** Some bridges have exposed steel gridwork embedded in the road, and certain highway turns have been roughened with rows of ridges to improve traction on wet days. Given that a car has 60-cm wheels, if the road ridges are 8.0 cm apart, at what speed will a vehicle traveling on such a surface go into resonance if the natural frequency of its “front end” (steering and suspension system) is 15.0 Hz?

**Solution:** [Given:  $D = 60$  cm,  $d = 8.0$  cm, and  $f_0 = 15.0$  Hz. Find:  $v$  for resonance.] There are  $1/0.080 =$

12.5 ridges per meter and so at speed  $v$  (in m/s), the car is moving over 12.5 $v$  ridges per second, which is the driving frequency. Hence

$12.5v = 15.0$  Hz  
and  $v = 1.2$  m/s or 3 mi/h, regardless of wheel size. That's why your car shakes so much at low speeds on that kind of surface.

**Quick Check:**  $v = x/T = x/(1/f_0) = (0.080 \text{ m}) / (15.0 \text{ Hz}) = 1.2 \text{ m/s}$ .

Tap a good quality wineglass and it will ring, undriven, at its natural frequency, somewhere around 900 Hz. If it's now forced at that frequency, for example, by a blast of vibrating air (that is, sound) up near the rim, the glass will efficiently ab-

**This Page is Inserted by IFW Indexing and Scanning  
Operations and is not part of the Official Record**

**BEST AVAILABLE IMAGES**

Defective images within this document are accurate representations of the original documents submitted by the applicant.

Defects in the images include but are not limited to the items checked:

- ☒ **BLACK BORDERS**
- ☐ **IMAGE CUT OFF AT TOP, BOTTOM OR SIDES**
- ☐ **FADED TEXT OR DRAWING**
- ☐ **BLURRED OR ILLEGIBLE TEXT OR DRAWING**
- ☐ **SKEWED/SLANTED IMAGES**
- ☐ **COLOR OR BLACK AND WHITE PHOTOGRAPHS**
- ☒ **GRAY SCALE DOCUMENTS**
- ☒ **LINES OR MARKS ON ORIGINAL DOCUMENT**
- ☐ **REFERENCE(S) OR EXHIBIT(S) SUBMITTED ARE POOR QUALITY**
- ☐ **OTHER: \_\_\_\_\_**

**IMAGES ARE BEST AVAILABLE COPY.**

**As rescanning these documents will not correct the image problems checked, please do not report these problems to the IFW Image Problem Mailbox.**